AD_____

Award Number:

W81XWH-05-1-0115

TITLE:

Angiogenesis and Tissue Engineering Research

PRINCIPAL INVESTIGATOR:

Donald Ingber, M.D., Ph.D.

CONTRACTING ORGANIZATION:

Children's Hospital
Boston, MA 02115

REPORT DATE:

August 2010

TYPE OF REPORT:

Final Addendum

PREPARED FOR: U.S. Army Medical Research and Materiel Command
Fort Detrick, Maryland 21702-5012

DISTRIBUTION STATEMENT:

X Approved for public release; distribution unlimited

REPORT DOCUMENTATION PAGE

Form Approved
OMB No. 0704-0188

1. REPORT DATE *(DD-MM-YYYY)*	2. REPORT TYPE	3. DATES COVERED *(From - To)*
01-08-2010	Final Addendum	24 MAR 2009 - 31JUL 2010

4. TITLE AND SUBTITLE

Angiogenesis and Tissue Engineering Research

5a. CONTRACT NUMBER

5b. GRANT NUMBER
W81XWH-05-1-0115

5c. PROGRAM ELEMENT NUMBER

6. AUTHOR(S)
Donald Ingber, M.D., Ph.D., Mark Puder, M.D., Ph.D., Joyce Bischoff, Ph.D.

5d. PROJECT NUMBER

5e. TASK NUMBER

5f. WORK UNIT NUMBER

7. PERFORMING ORGANIZATION NAME(S) AND ADDRESS(ES)

Children's Hospital

Boston, MA 02115

8. PERFORMING ORGANIZATION REPORT NUMBER

9. SPONSORING / MONITORING AGENCY NAME(S) AND ADDRESS(ES)

U.S. Army Medical Research and Materiel Command
Fort Detrick, Maryland 21702-5012

10. SPONSOR/MONITOR'S ACRONYM(S)

11. SPONSOR/MONITOR'S REPORT NUMBER(S)

12. DISTRIBUTION / AVAILABILITY STATEMENT

Approved for public release; distribution unlimited

13. SUPPLEMENTARY NOTES

14. ABSTRACT

Project I: Centers on the development of new medical therapies and regenerative medicine approaches for the treatment of injured soldiers, and the improvement of the overall health and performance of military personnel. Over the past year we designed to develop aerosol therapies to save lives in patients with pulmonary edema and Acute Respiratory Distress Syndrome (ARDS; we evaluated the anti-malarial activity of an oral angiogenesis inhibitor developed in past grant funding periods, called Lodamin, that is a methionine aminopeptidases 2 (MetAP2)inhibitor; and, we developed new microsystems technologies to harvest rare circulating stem cells for tissue engineering applications, such as blood vessel precursor cells for tissue revascularization. Project II: Adhesions are a major source of morbidity in surgical and gynecological patients, and we have previously shown that murine intra-abdominal adhesions are prevented with the angiogenesis inhibitor Sutent®. The dosage of Sutent® has been established at 10mg/kg/day based on previous experiments. The treatment duration required to prevent adhesion formation and avoid potential adverse reactions was recently determined. With the optimal treatment duration established, the bursting strength of bowel anastomoses and the tensile strength of incisional abdominal wounds were evaluated. In addition, in determining the efficacy of angiogenesis inhibitors, we are currently evaluating the effect of Sutent® on uterine function following uterine abrasion and adhesion formation.Following completion of the animal studies, we will focus on establishing a multi-center clinical trial to evaluate anti-angiogenic medications on adhesion formation. Project III: We have shown that human endothelial progenitor cells (EPCs) and mesenchymal progenitor cells (MPCs) can be isolated from blood or bone marrow, expanded ex vivo and used to build new vascular networks in vivo. Our specific objectives for the past year have been to 1) improve methods for isolating and expanding human MPCs, 2) to determine if EPCs and MPCs can be isolated from cryopreserved blood samples and 3) to determine if EPCs and MPCs can form vascular networks in regenerating tissues. Objective 3 represents an important culmination of this DOD sponsored research because it will be important to determine whether or not EPCs and MPCs can form functional blood vessels in a relevant tissue or organ setting; this will be an important step beyond our well-established but somewhat artificial Matrigel model.

15. SUBJECT TERMS Lodamin, TNP470, doxycycline, Bevacizumab, endostatin, pulmonary edema, acute respiratory distress syndrome, malaria, microfluidics, magnetic separations, stem cell isolation, angiogenesis inhibitors, intra-abdominal adhesions, abdominal trauma, wound strength, bowel anastamosesendothelial progenitor cells, mesenchymal cells, tissue-engineering, microvasculature,angiogenesis, skin grafts, microfluidics

16. SECURITY CLASSIFICATION OF:			17. LIMITATION OF ABSTRACT	18. NUMBER OF PAGES	19a. NAME OF RESPONSIBLE PERSON
a. REPORT	b. ABSTRACT	c. THIS PAGE			USAMRMC
U	U	U	UU	43	19b. TELEPHONE NUMBER *(include area code)*

Table of Contents

Project I:

Project II:

Project III:

DOD Congressional Annual Report *(04/24/09 – 04/23/10)*

PROJECT 1: Vascular Therapies for Military Casualties

Donald Ingber, M.D., Ph.D. *Principal Investigator*
Benjamin Matthews, M.D., *Co-Principal Investigator*
Akiko Mammoto, M.D., Ph.D., *Research Associate*
Robert Mannix, Ph.D., *Research Fellow*
Chong Yung, Ph.D., *Research Fellow*
Joo Kang, Ph.D., *Research Fellow*
Umai Kanapathipillai, Ph.D., *Research Fellow*
Ryan Cooper, *Graduate Student*
Heather Tobin, *Veterinary Technician*
Merina Shakya, *ResearchTechnician*
Tracy Tat, *Research Technician*

I. ABSTRACT

Our project, which involves 3 major Tasks, centers on the development of new medical therapies and regenerative medicine approaches for the treatment of injured soldiers, and the improvement of the overall health and performance of military personnel. Over the past year in studies in our first Task, we designed to develop aerosol therapies to save lives in patients with pulmonary edema and Acute Respiratory Distress Syndrome (ARDS), which are major causes of death and morbidity in patients with trauma. In the second Task, we evaluated the anti-malarial activity of an oral angiogenesis inhibitor developed in past grant funding periods, called Lodamin, that is a methionine aminopeptidases 2 (MetAP2)inhibitor. In our last Task, we developed new microsystems technologies to harvest rare circulating stem cells for tissue engineering applications, such as blood vessel precursor cells for tissue revascularization, as described in Project 3. These devices may also be useful for isolating circulating cancer cells and so facilitate new approaches to cancer diagnosis and therapy.

II. INTRODUCTION

Over the past year, we have made major advances on all 3 Tasks. While past work focused on the studies of effects of angiogenesis modulators on permeability in the peripheral vasculature, we focused our efforts on establishing a mouse ex vivo ventilation perfusion model for analysis of lung trauma and quantitation of its effects of vascular permeability, pulmonary edema and inflammation. We also developed a novel miniaturized method for nebulizing drugs and nanoparticles and delivering aerosols containing these agents in the mouse. In addition, we identified a new molecular pathway that regulates the effects of physical forces on lung permeability. In the second Task, we carried out animal studies to explore whether the angiogenesis inhibitor, Lodamin, could be used as an oral therapeutic for soldiers and patients with malaria, which remains one of the most critical challenges in medicine today world-wide. The active moiety of Lodamin, TNP-470, inhibit MetAP2 activity and recently were reported to possess antimalarial activity in-vitro[1]; however, TNP-470 has poor bioavailability and therefore has to be admintered by infusion. Lodamin is a conjugate of TNP-470 with the block copolymer Polyethylene Glycol and Poly Lactic acid (PEG-PLA-TNP-470) that is orally available[2]. Over the past year, we evaluated the effect of Lodamin and TNP-470 on malarial growth and infection in vitro and in vivo in mice. Finally, in the last Task, we have used microengineering approaches to develope combined microfluidic-microfluidic devices that can isolate rare cells that are

circulating in whole blood. These devices may be used to harvest circulating stem cells from a soldier's blood to facilitate the vascular regeneration effort being pursued by Dr. Bischoff in Task 3 of this grant. We also developed devices that can rapidly isolate circulating cancer cells, which might be useful for diagnosis and therapy of patients with cancer.

III. BODY:

As outlined in the Statement of Work, our research accomplishments this past year in Project 1 include the following:

Task 1: Therapies for Lung Vascular Injury

During the past year, we established an *ex vivo* mouse lung ventilation-perfusion model in our laboratory, developed a specialized intratracheal nebulization catheter to introduce aerosols into the lungs of mice[3], and modified this system to include real time monitoring of mouse lung weight during *ex vivo* ventilation perfusion. We then investigated the effects of barotrauma (high pressure mechanical ventilation) on pulmonary edema and lung inflammation using this model. We found that lung trauma significantly increased pulmonary edema as illustrated by increased vascular permeability (Kf) and whole lung wet values (Fig. 1). Lung sections and fluid samples from these studies will soon be analyzed to quantitate separate measures of pulmonary edema and inflammation. In addition, we have begun to study the effect of pre-treating mice with intraperitoneal injections of IL-2 in order to induce inflammation and pulmonary edema prior to the initiation of mechanical ventilation. Finally, we used the ex vivo model to confirm the prediction that mechanical breathing movements enhance absorption of aerosolized nanoparticles, as predicted by a microengineered breathing lung-on-a-chip microdevice that was developed in collaborative studies[3].

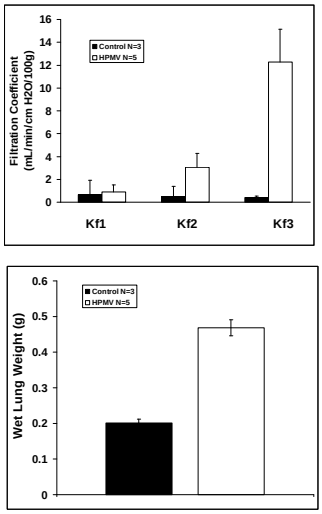

Fig. 1. Effects of lung trauma induced by high pressure mechanical ventilation (HPMV) on whole lung vascular permeability (top) and weight (bottom).

In addition, based on our recent finding that the extracellular matrix (ECM) mechanics mediate blood vessel formation *in vivo*by altering changes in signaling through p190RhoGAP and the transcription factors TFII-I and GATA2[4], we initiated studies to explore whether ECM mechanics also control vascular permeability in human lung microvascular endothelial cells. We found that knockdown of the mechanosensitive transcription factor TFII-I using siRNA-based knockdown disrupted cell-cell junctions and increased the vascular permeability using an *in vitro* permeability assay, whereas overexpression of TFII-I using lentivirus transduction had opposite effects. We also found that TFII-I knockdown increased the mouse lung vascular permeability *in vivo*. Importantly, changes in ECM stiffness controlled cell-cell junction structures detected by VE cadherin staining: these junctions were well developed in cells on stiff gels (4000 Pa), whereas they were disrupted on the soft gels (150 Pa). TFII-I knockdown disrupted cell-cell junctions on stiff gels (4000 Pa) and TFII-I overexpression restored the junctional integrity on soft gels (150 Pa), suggesting that TFII-I mediates mechanical control of endothelial cell-cell junction formation and hence control vascular permeability *in vivo*. These findings may provide some insight into the mechanism by which physical forces and trauma influence lung vascular leakage.

Task 2: Development of a new-Anti Malarial Therapy

Lodamin (PEG-PLA-TNP-470) was synthesized and provided to collaborators at the Harvard School of Public Health, Broad Institute and Genzyme Inc. for studies to test Malaria growth in an *in vitro* blood cell infection model as well as a mouse model of malaria infection. Preliminary data showed that Lodamin significantly inhibited parasite viability in vitro at doses of 2-10nM, suggesting that it is slightly more potent than the parent compound TNP-470. In the mouse studies, 5 animals were dosed orally b.i.d. with 30 mg/kg Lodamin for 4 days. On day 5 mice were sacrificed and blood sample from each mouse were taken for thin smears. A significant reduction of 61% in parasites counted in smears was observed in Lodamin-treated mice compared to controls (Fig. 2). To facilitate these studies, we also developed an analytical method for quantitation of the amount of drug (TNP-470) in the plasma using LC/MS/MS and MALDI TOF techniques. Since numerous peaks were detected in mass spectrometry due to Lodamin fragmentation (polymer degradation), we are currently optimizing the Lodamin sample preparation for detection of TNP-470 in plasma with increased accuracy. Once this method is established, we plan to design and conduct a study to determine the maximum tolerated dose (MTD) necessary to achieve sterile cure in the *in vivo* mouse malaria model.

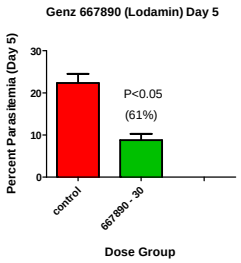

Fig. 2. Lodamin inhibit parasite count in mice. A dose of 30mg/kg of oral Lodamin was administered for 4 days. At day 5th parasite count in the blood smears originated from the different mice were performed. Untreated mice were used as controls.

Task 3: Microengineering methods for harvesting rare circulating cells

Endothelial progenitor cells (EPCs) are promising sources of cells for angiogenic therapies because they contribute to new blood vessel formation, as described in Project 3 of this grant; however, efficient isolation of EPCs from circulating blood remains a significant obstacle due to their low numbers. We used microengineering approaches to develop a combined microfluidic-micromagnetic system for isolating EPCs from human blood with great efficiency. We made great improvements to the prototype device described in last year's annual report by incorporating double-protection channels and dead-end channels to sequester magnetic bead-labeled cells. To determine the quantitative efficiency of the device, we spiked whole human blood or culture medium with known numbers of green fluorescence protein (GFP)-expressing human umbilical vein endothelial cells (HUVECs) before combining them with magnetic beads coated with antibodies to CD31 and passing them through the micromagnetic-microfluidic collection device. We found that virtually all (~100%) of the cells were removed from the blood magnetically, and that ~1-2 x10^5 cells were retained in each device; however, only 60 – 80% of the separated cells could be removed from the device and collected (Fig. 3). Development of improved methods to wash collected cells free from the device will be a key goal in further studies. In addition, we found that EPCs can be isolated from the buffy coat fraction of whole blood (obtained from the Children's Blood Bank) using standard filter isolation methods used by the Bischoff lab, and that the isolated cells grown in culture and form classic EPC colonies. Thus, we plan to use human buffy coats isolated in this clinically approved manner as an

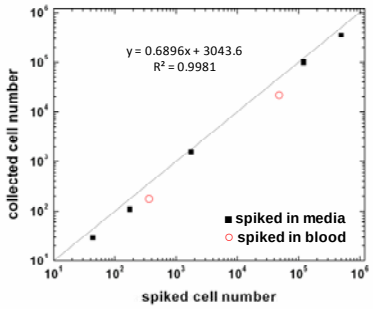

Fig. 3. A plot showing the collection efficiency of the microfluidic device comparing the number of the cells spiked in the blood (X-axis) versus the number of the cells collected from the device (Y-axis). Line indicates100% collection efficiency; black squares and red circles represent the results of the GFP-HUVECs spiked in medium and whole blood, respectively.

EPC source in future cell isolation studies. Interestingly, in collaborative studies, we also discovered that the same device can be used to harvest rare circulating tumor cells in a mouse transgenic breast cancer model, and hence this method might facilitate cell isolation for diagnosis, therapy or vaccine development in patients with cancer in the future.

IV. KEY RESEARCH ACCOMPLISHMENTS:

Task1-

- Developed an *ex vivo* mouse lung ventilation-perfusion model that mimics the effects of barotraumaon pulmonary edema
- Used the ex-vivo mouse lung ventilation perfusion model to confirm predictions of a new 'lung-on-a-chip' microdevice that recapitulates key physiological responses of the lung alveolar-capillary unit.
- Discovered that transcription factorTFII-I and changes in ECM stiffness control vascular permeability in the mouse.

Task 2-

- Demonstrated anti-malaria effect of oral Lodamin in a mouse malaria model
- Developed an analytical method for testing the Lodamin efficacy in vivo

Task 3-

- Developed a microfluidic-micromagnetic device that enables efficient capture of rare circulating cells from human blood
- Demonstrated that we might harvest EPCs using this method with buffy coat isolates in the future
- Demonstrated that this device can provide efficient capture of rare circulating tumor cells in a mouse transgenic breast cancer model

V. REPORTABLE OUTCOMES:

- Huh D, Matthews BD, Mammoto A, Montoya-Zavala M, Hsin HY, and Ingber DE. Reconstituting Organ-Level Lung Functions on a Chip. *Science* – in press.
- Additional manuscripts on TFII-I and pulmonary edema, and on cell isolation methods are in preparation
- A patent is in the process of being prepared on the cell isolation microdevice
- Biomedical Engineering Society (BMES) Pritzker Distinguished Lectureship Award
- *Charlton Lecture*, Tufts University School of Medicine
- Rous Whipple Award, American Society for Investigative Pathology
- Llewellyn-Thomas Visiting Professor, U. of Toronto

VI. CONCLUSIONS:

We have established robust mouse model of barotrauma-induced lung injury in our laboratory that can be used in the future to test the ability of aerosolized drugs and nanoparticles for treatment and prevention of life-threatening pulmonary edema and ARDS that takes the lives of many injured soldiers. We also demonstrated that the oral angiogenesis inhibitor and MetAP2 inhibitor, Lodamin, can suppress malarial infection in an animal model; however, dose optimization and mean tolerated dose studies need to be completed before its full value can be determined. Finally, we have developed simple microdevices that offer a novel method for efficiently isolating rare circulating cells from human blood or buffy coats (white

blood cell isolates). This method might be very useful for isolation of circulating EPCs or mesenchymal stem cells that are critical for regenerative medicine applications, and the same device might be used to isolate circulating tumor cells for cancer diagnosis, therapeutic sensitivity testing and vaccine development in the future.

"So What Section"

Vascular leakage in the lung and resulting pulmonary edema caused by trauma is a major cause of morbidity and death in injured soldiers and thus, developing new therapeutics to treat or prevent this response could save lives. The ex vivo mouse model we have developed will now enable us to test the ability of angiogenesis modulators and other therapeutics to suppress these responses, and therefore hopefully accelerate development of life-saving therapies. The angiogenesis inhibitor Lodamin is well tolerated in animals, and the parent agent TNP-470 has been tested without serious adverse effects in humans. Thus, if this oral agent is found to be active as a anti-malarial therapeutic, it could be used as a prophylactic agent in soldiers stationed in regions where malaria is indigenous, and it also could be used as a new therapy world-wide. Finally, the microdevices we developed for isolation rare circulating cells from blood can be used to harvest many types of cells, including EPCs, mesenchymal stem cells, hematopoietic stem cells, tumor cells, and pathogens, among others. Thus, this microfluidic platform could facilitate development of new strategies for patient-specific therapies for tissue regeneration, as well as cancer, sepsis and other life-threatening diseases.

VII. REFERENCES:

1. Chen X, Xie S, Bhat S, Kumar N, Shapiro TA, Liu JO. Fumagillin and Fumarranol Interact with P. falciparum Methionine Aminopeptidase 2 and Inhibit Malaria Parasite Growth In Vitro and In Vivo..*Chem Biol.* 2009 Feb 27;16(2):193-202.
2. Benny O, Fainaru O, Adini A, Cassiola F, Bazinet L, Adini I, Pravda E, Nahmias Y, Koirala S, Corfas G, D'Amato RJ, Folkman J. An orally delivered small-molecule formulation with antiangiogenic and anticancer activity. *Nature Biotechnol.* 2008 Jul;26(7):799-807. Epub 2008 Jun 29.
3. Mammoto A, Connor K, Mammoto T, Aderman C, Mostoslavsky G, Smith LEH and Ingber DE. A mechanosensitive transcriptional mechanism that controls angiogenesis. *Nature* 2009; 457, 1103-1008.
4. Huh D, Matthews BD, Mammoto A, Montoya-Zavala M, Hsin HY, and Ingber DE. Reconstituting Organ-Level Lung Functions on a Chip. *Science* – in press.

VIII. APPENDICES:

None

Project II: The Prevention of Post-operative and TraumaticAbdominal Adhesions

Mark Puder, M.D. Ph.D., *Primary Investigator*
Erica Fallon, M.D., *Research Fellow*
Hau Le, M.D., *Research Fellow*
Jonathan Meisel, M.D., *Research Fellow*
Amy Pan, *Research Technician*

I. ABSTRACT:

Abdominal adhesions are a major source of morbidity in surgical and gynecological patients. We have previously shown that murine intra-abdominal adhesions are prevented with the angiogenesis inhibitorSutent®. We are currently utilizing a pre-clinical leporine model.Our specific objectives for the past year have been to 1) determine the optimal treatment duration of Sutent®; 2) evaluate the bowel bursting and incisional abdominal wound strengths following treatment with Sutent®; and 3) evaluate the effect of Sutent® on uterine function following uterine abrasion and adhesion formation. The dosage of Sutent®has been established at 10mg/kg/day based on previous experiments. The treatment duration required to prevent adhesion formation and avoid potential adverse reactions was recently determined. With the optimal treatment duration established, the bursting strength of bowel anastomoses and the tensile strength of incisional abdominal wounds were evaluated. In addition, in determining the efficacy of angiogenesis inhibitors, we are currently evaluating the effect of Sutent® on uterine function following uterine abrasion and adhesion formation.Following completion of the animal studies, we will focus on establishing a multi-center clinical trial to evaluate anti-angiogenic medications on adhesion formation.

II. INTRODUCTION:

Postoperative abdominal adhesions are a major cause of morbidity and mortality in general and gynecologic surgery patient populations. While adhesions are the number one cause of bowel obstructions and secondary infertility worldwide, they can lead to prolonged hospital stays and often additional abdominal operations. In fact, adhesions are responsible for approximately 1 million inpatient hospital days and $1 billion in hospital costs and healthcare resources yearly. Several approaches have been attempted to inhibit abdominal adhesion formation, although most with limited success [1, 2]. For adhesion prevention, we have focused on tyrosine kinase inhibitors,an FDA approved class of drugs with have both anti-angiogenic and anti-tumor properties. In clinical practice, these drugs are approved for use in advanced stages of renal cell carcinoma and imatinib-resistant gastrointestinal stromal tumors. Sunitinib (sunitinib malate, sutent®, SU11248; Pfizer) is a tyrosine kinase inhibitor which inhibits receptors for vascular endothelial growth factor(VEGF) and platelet derived growth factor (PDGF). VEGF has beendemonstrated to be upregulated in adhesion formation.Adhesions form as a result of altering the normal healing process and all tissues require angiogenesis for wound healing. If receptors of VEGF were inhibited using an angiogenic inhibitor, such asSutent®, we hypothesize that postoperative intraabdominal adhesions would be prevented or reduced.

III. BODY:

Objective: To determine the optimal treatment duration of Sutent® to prevent adhesions and avoid complications associated with the use of angiogenesis inhibitors.

In prior experiments we used 10 doses (10mg/kg/day), not including the pre-operative dose (10mg/kg), and found a significant reduction in postoperative abdominal adhesions. Following these results, we were interested in evaluating whether shorter treatment duration could prevent adhesions while avoiding potential complications associated with angiogenesis inhibitors. In the 1st quarter of 2009, we performed the uterine abrasion and bowel anastomosis procedures on 10 rabbits. Five animals were treated with 10 postoperative Sutent®doses compared to five non-treated animals. Treated animals had minimal to no adhesions compared to control animals (see photos below). To determine if altering the treatment duration could prevent adhesions while avoiding complications associated with angiogenesis inhibitors, the treatment duration was changed from 10 to 5 days, not including the 1 pre-operative dose (10mg/kg). We randomly treated 5 rabbits with an experimental dose of Sutent® 10mg/kg/day for 5 days postoperatively while the remaining rabbits were treated with saline (control). All rabbits survived the procedure and were sacrificed on postoperative day 10. Adhesions were gradedand abdominal wounds were collected for further analysis. On sacrifice, the animals treated with 5 days of Sutent®had greater percentage and tenacity of adhesions compared to those animals treated with 10days of Sutent®(from prior experiments). Total adhesion scores were calculated for each rabbit by combining the tenacity and percentage score, as previously described. See Figure 1 (next page). These results were encouraging, yet suboptimal.

Following the 5-day treatment trail, we chose to evaluate an 8-day treatment duration. We randomly treated 5 rabbits with an experimental dose of Sutent® 10mg/kg/day for 8 postoperative days while the remaining rabbits were treated with saline. We then repeated the initial 10-day experiment using Sutent® 10mg/kg/day; the experiment included 9 treated animals (1 rabbit died due to complications of orogastric gavage) and 10 control animals. All animals were sacrificed on post-operative day #10, adhesions were graded and abdominal wounds were collected. Total adhesion scores were calculated for each rabbit by combining the tenacity and percentage score, as previously described. Findings revealed the animals treated with 8 days of Sutent®had greater percentage and tenacity of adhesions compared to those animals treated with 10 days of Sutent®. See Figure 1 (next page).

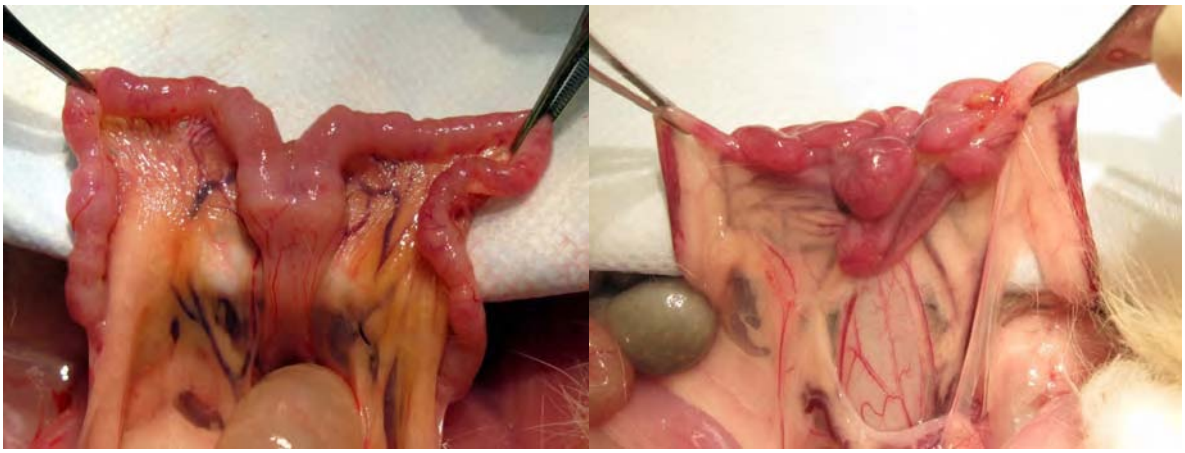

Treated Animal (Sutent x10d) Control Animal

Figure 1: <u>Total Adhesion Score</u>: <u>10d v 5d v 8d Treatment Duration</u>

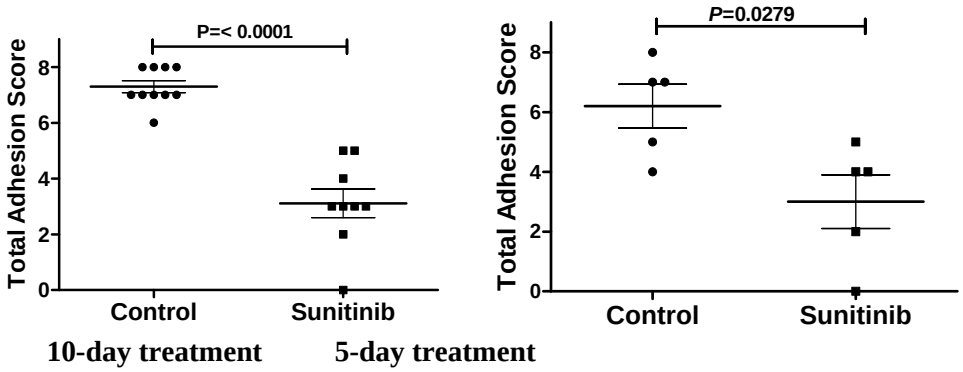

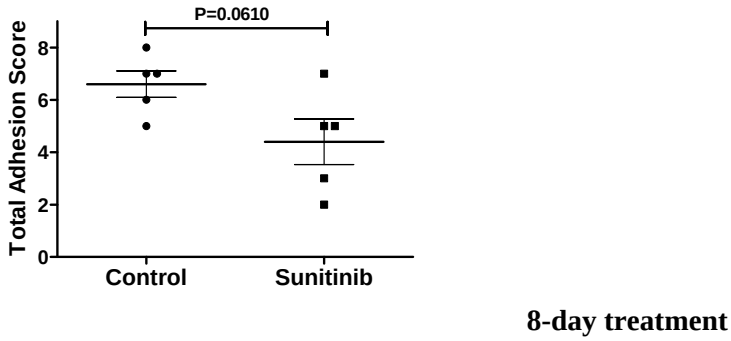

<u>Objective</u>: To evaluate the intestine and incisional abdominal wound strengths following treatment with Sutent.

The bursting strength of intestinal anastomoses was evaluated to determine if Sutent® has an effect on intestinal healing. In the 10d vs 5d experiment, we evaluated bursting strength using a previously established model [3]. The segment of bowel with the anastomosis was occluded on one end with a bowel clamp while the other end was cannulated with infusion tubing and held in place. Pressure transducer tubing was inserted distal to the anastomosis and attached to a monitor (Surgivet V9212AR, Waukesha, WI, USA). Water was then slowly infused into the bowel and the pressure at which the bowel burst was manually recorded. Preliminary

results demonstrated a decreased bursting strength in Sutent® treated animals compared to controls, regardless of treatment period (10d vs 5d). At the time of sacrifice, the anastomoses were inspected and there was no evidence of disruption or leak in any animal. See Figure 3 below.

The tensile strength of abdominal wounds was evaluated to determine if Sutent® has a deleterious effect on wound healing. For ultimate tensile strength measurements, wounds were analyzed inuniaxial tension on a screw-driven Instron 5542 Load Frame with a 500N load cell (Instron, Canton, MA) at a constant strain rate of 0.001/s. Results of wound tensile strength are shown in Figure 3.

Figure 2: Bowel Bursting Strength

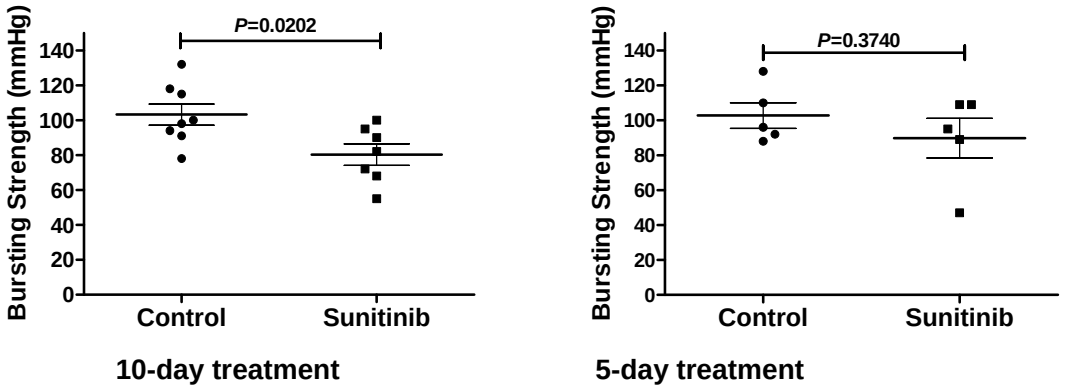

Figure 3: Wound Tensile Strength

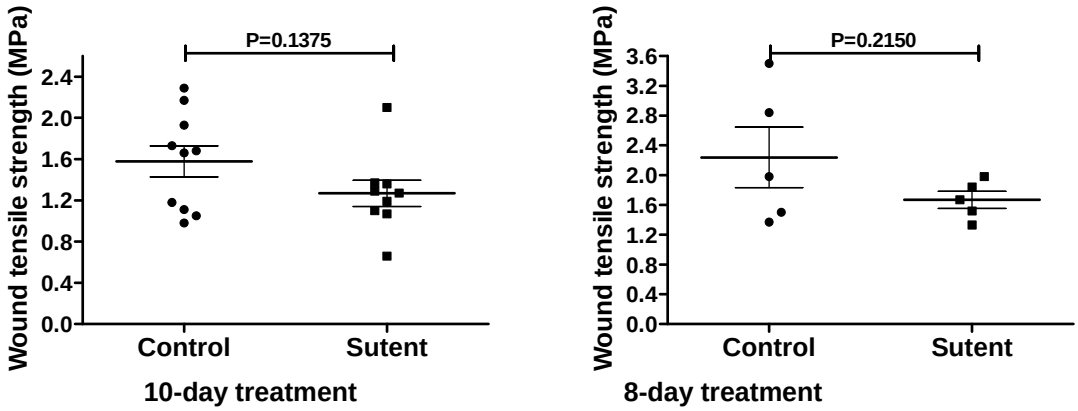

Objective: To evaluate the effect of Sutent® on uterine function following uterine abrasion and adhesion formation

To determine the efficacy of angiogenesis inhibitors, we proposed to evaluate the effect of Sutent®on uterine function following uterine abrasion and adhesion formation. Uterine function, defined as the ability to conceive, gestate, and deliver offspring, will serve as the primary outcome measure in the evaluation of anti-angiogenic treatment on adhesion formation following abdominal surgery in rabbits. In order to evaluate functionality, we requested approval (within the no-cost extension) to breed animals, and then monitor and follow pregnant animals

through gestation and delivery. Breeding occurs following the uterine abrasion procedure and randomized treatment with Sutent®*vs* vehicle for 10 postoperative days, a duration previously shown to prevent adhesion formation in these animals.

Preliminary results demonstrate that treatment with Sutent®does *not* affect the breeding pattern (e.g gestation, uninterrupted delivery), normal development of the fetus, litter size, and / or maintenance of normal maternal behaviors. Treated animals have minimal to no adhesions on necropsy compared to untreated animals with multiple areas of adhesed tissue. Ultrasound images of fetuses are displayed below, in addition to uteruses post-delivery in treated vs untreated animals.

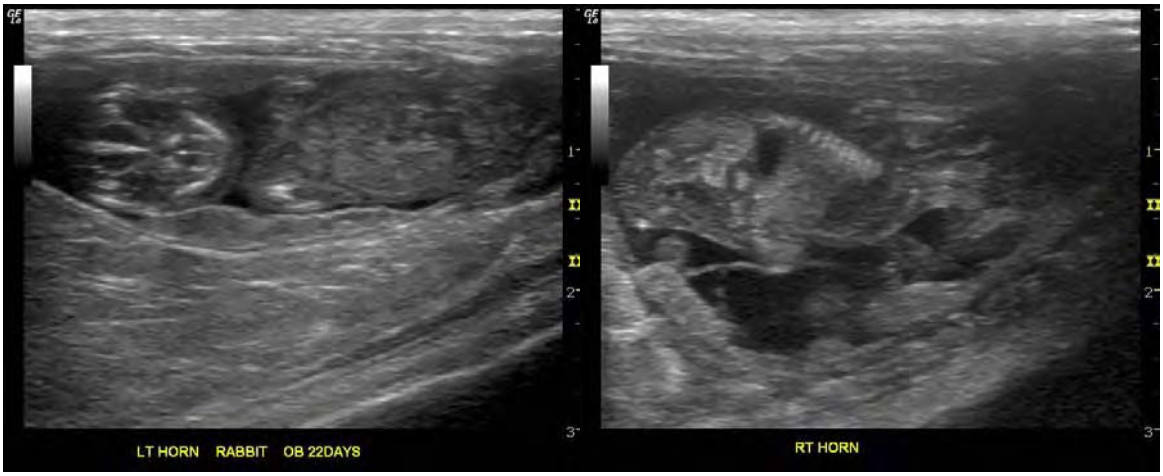

Fetus in Left Uterine Horn Fetus in Right Uterine Horn

Uterus from Treated Animal Uterus from Untreated Animal

IV. KEY RESEARCH ACCOMPLISHMENTS:

1. The optimal dosage and treatment duration of Sutent®are 10mg/kg/d and 10 postoperative days, respectively.
2. Sutent® appears to decrease bowel bursting strength in treated vs untreated animals
3. There is no significant difference in wound tensile strength between groups
4. Based on preliminary results, Sutent® administration following uterine abrasion and before parturition does not appear to affect breeding pattern, fetal development or maintenance of maternal behaviors.

V. REPORTABLE OUTCOMES:

Manuscript: Meisel JA, Le H, de Meijer VE, Puder M. *Sunitinib Inhibits Postoperative Adhesions in a Large Animal Model*. To be submitted to British Journal of Surgery.

Presentation: Meisel JA, Le HD, de Meijer, VE, Puder M. *Inhibition of Intra-abdominal Adhesion Formation in a Rabbit Model with the Angiogenesis Inhibitor Sunitinib*. American Pediatric Surgical Association – 40th Annual Meeting, Fajardo, Puerto Rico, May 2009.

Abstract: Fallon EM; Le HD, de Meijer VE, Puder, M. *Effect of Anti-Angiogenic Therapy on Adhesion Formation and Functional Outcome in a Leporine Model*. Submitted to the American College of Surgeons Annual Meeting, October 2010.

VI. CONCLUSIONS:

Sutent® has been shown to significantly reduce postoperative adhesions in murine [4] and leporine models. The use of angiogenesisinhibitors may be an efficacious strategy to prevent or treat adhesions following abdominal procedures and improve related morbidity and mortality. In addition, anti-angiogenic therapy may be beneficial in maintenance of reproductive uterine function with elimination of adhesion-related uterine complications. Future work will be directed towards clinical trial development.

"So What Section"

Adhesions are the major cause of intestinal obstruction, which can lead to prolonged hospital stays and often additional abdominal operations, which perpetuates the problem itself. Adhesions also increase the morbidity and mortality of each subsequent operation because they lead to increased blood loss and injury to internal organs. In the United States, the total cost from complications from adhesions is over $1 billion a year, and accounts for over 846,000 inpatient care days [5]. The prevention of adhesions would profoundly decrease the morbidity and reduce health care costs across a broad range of medical disciplines [6].

VII. REFERENCES:

1. Montz FJ, Holschneider CH, Bozuk M, Gotlieb WH, Martinez-Maza O (1994) Interleukin 10: ability to minimize postoperative intraperitoneal adhesion formation in a murine model. Fertil Steril 61: 1136-1140.

2. Rodgers KE, Johns DB, Girgis W, Campeau J, diZerega GS (1997) Reduction of adhesion formation with hyaluronic acid after peritoneal surgery in rabbits. Fertil Steril 67: 553-558.

3.de Hingh IH, de Man BM, et al. (2003). Colonic anastomotic strength and matrix metalloproteinase activity in an experimental model of bacterial peritonitis. Br J Surg 2003;90(8):981-8.

4. Kim S, Lee S, Greene AK, Arsenault DA, Le H, Meisel J, Novak K, Flynn E, Heymach JV, Puder M (2008) Inhibition of intra-abdominal adhesion formation with the angiogenesis inhibitor sunitinib. J Surg Res 149(1):115-9.

5. Ray NF, Denton WG, Thamer M, Henderson SC, Perry S (1998) Abdominal adhesiolysis: inpatient care and expenditures in the United States in 1994. J Am Coll Surg 196: 1-9.

6. Menzies D, Parker M, Hoare R, Knight A (2001) Small bowel obstruction due to postoperative adhesions: treatment patterns and associated costs in 110 hospital admissions. Ann R Coll Surg Engl 83: 40-46.

VIII. APPENDICES:

None

Project III: New Blood Vessels using Blood-derived Endothelial and Mesenchymal Progenitor Cells

Joyce Bischoff, Ph.D., *Principal Investigator*
Nasreen Bashir, Ph.D., *Research Fellow*
Elisa Boscolo, Ph.D., *Research Fellow*
Kyu-Tae Kang, Ph.D., *Research Fellow*
Jill Wylie-Sears, Ph.D., *Research Technologist*

I. ABSTRACT:

We have shown that human endothelial progenitor cells (EPCs) and mesenchymal progenitor cells (MPCs) can be isolated from blood or bone marrow, expanded ex vivo and used to build new vascular networks in vivo[1, 2]. The robust vasculogenesis (defined as de novo blood vessel formation from progenitor cells) that can be achieved using normal human cells has brought us closer to our goal of building blood vessel networks from human progenitor cells obtained without sacrifice of healthy tissues, veins or arteries.

Our specific objectives for the past year have been to 1) improve methods for isolating and expanding human MPCs, 2) to determine if EPCs and MPCs can be isolated from cryopreserved blood samples and 3) to determine if EPCs and MPCs can form vascular networks in regenerating tissues. In regard to Objective 3, during the past two months we have pursued a liver regeneration model in collaboration with Dr. Puder's laboratory, because initial studies with vascularizing skin constructs were not successful. Specific details of our progress are described below. Objective 3 represents an important culmination of this DOD sponsored research because it will be important to determine whether or not EPCs and MPCs can form functional blood vessels in a relevant tissue or organ setting; this will be an important step beyond our well-established but somewhat artificial Matrigel model.

In studying the time course of blood vessel formation in the Matrigel model, we discovered a transient incursion of myeloid cells into the Matrigel, and demonstrated a functional role for these cells[3]. This provides important information about the role of host cells in facilitating vessel formation. The work was published in Tissue Engineering in March 2010[3]. A pdf is included in the report.

II. INTRODUCTION:

Our goal is to build vascular networks from human endothelial progenitor cells (EPCs) and mesenchymal progenitor cells (MPCs) to re-vascularize damaged tissues and organs. We envision use of a soldier's own EPCs and MPCs for a variety of tissue-engineering (TE) applications and for tissue regeneration. For TE, vascular networks created from EPCs/MPCs would be incorporated into TE constructs in vitro such that upon implantation in vivo, anastomoses with the host circulation would occur rapidly to establish blood flow. For tissue regeneration in situ, EPCs/MPCs would be delivered to the site in vivo where they would undergo vasculogenesis, as we have demonstrated can occur in vivo in our Matrigel-based model system. Our overall hypothesis is that EPCs and MPCs applied to either a TE organ or to regenerating ischemic tissue will establish an adequate blood supply and thereby promote resident cells to undergo appropriate tissue development and regeneration. We are testing this hypothesis in a liver regeneration model with Dr. Puder's laboratory (Objective 3).

III. BODY:

We envision that the beneficiary population would be patients/soldiers with injuries that require new tissue and/or regeneration. Soldiers are well-suited to this proposed strategy because our studies have shown that EPCs can be isolated from adult peripheral blood and MPCs can be isolated from adult bone marrow. Therefore, the cells needed to build new blood vessels can be isolated without sacrifice of healthy tissue and would be autologous cells, and thus immune-compatibility would not be a concern. New results performed for Objective 2, and results from Dr. Juan Melero-Martin's laboratory, show that EPCs can be isolated from cryopreserved blood samples. This establishes that blood samples could be stored frozen with only minimal preparation. EPCs and MPCs could then be isolated at a later date, if and when they were needed, to treat the soldier. Furthermore, there are new reports in the literature showing the increasing ease with which EPCs and MPCs can be isolated from relatively small blood or bone marrow samples, and that EPCs can be obtained from adults up to age 60, even from individuals with cardiovascular disease[4, 5]. In summary, there is now strong evidence from multiple laboratories that demonstrate 1) the ability to isolate and expand EPCs from adult blood and MPCs from adult bone marrow and 2) the ability of these two cells to form functional blood vessels in vivo in implanted gels of extracellular matrix. The critical, next step will be to determine if functional vascular networks can be formed in an ischemic or regenerating tissue and if this results[6] in improved outcomes.

To address this, we are collaborating with Dr. Puder's lab to pursue the goals of Objective 3 using a liver regeneration model that his laboratory has pioneered[6]. The important attributes that make the liver regeneration model particularly useful are 1) less tissue necrosis after partial hepatectomy and 2) immediate initiation of liver regeneration without any complications of inflammatory reactions. Preliminary results in this model are shown below.

Objectives:

Objective 1 - Determine if we can isolate mesenchymal progenitor cells (MPCs) from adult peripheral blood.
Dr. Nasreena Bashir has identified Mesencult Media (Stem Cell Technologies) as advantageous for isolating and expanding human MPCs. We are continuing to test this media for isolating MPCs from adult peripheral blood.

Objective 2 - Cryopreserve mononuclear cells (MNCs) to determine if EPCs and MPCs can be isolated from a previously frozen aliquot of human MNCs.
Dr. Bashir has shown that umbilical cord blood samples can be processed to obtain a nucleated cell fraction and cryopreserved in three different types of typical solutions for cryopreservation. After storage in liquid nitrogen for 1 or 3 months, samples were thawed and EPCs were readily obtained. A thorough analysis of EPCs obtained from cryopreserved blood cells has been conducted by Dr. Juan Melero-Martin, and he has submitted a manuscript for publication. Therefore, this objective has been achieved for EPCs.

Objective 3 - Test ability of human EPCs and MPCs to migrate into human skin equivalents and form vascular structures.
We do not have data to report on this but as described in the introduction, we submitted and received approval (and funds) to test the ability of EPCs and MPCs to form functional vascular networks in a liver and pancreatic regeneration models in collaboration with Dr. Puder's laboratory.

We hypothesize that delivery of EPCs and MPCs to animals undergoing organ regeneration will accelerate regeneration by providing building new blood vessels and providing increased perfusion to the regenerating organ. If this hypothesis is correct, delivery of EPCs/MPCs could be developed as a novel cell-based strategy for enhancing organ regeneration in soldiers with organ or tissue damage.

Figure 1 shows preliminary data from the liver regeneration model. The first experiments have been directed at tracking EPCs alone and EPCs combined with MPCs after tail vein injection into mice that received partial hepatectomy. EPCs were labeled with firefly luciferase to enable tracking by bioluminescence imaging. Three experiments have been conducted thus far. The preliminary results in Figure 1 show a bioluminescence signal (blue/turquoise) in ¾ mice injected with EPCs and MPCs. The variability of the signal among the different animals is under investigation. After Day 7, livers were harvested and half of each was saved to measure the luciferase activity and the remaining half was stained for EPC and MPC markers with antibodies against human antigens. We are encouraged by this data and will continue with this Objective for the remainder of the funding period.

IV. KEY RESEARCH ACCOMPLISHMENTS:

1. Published paper showing the transient influx of myeloid cells into Matrigel implants at 2-3 days after in vivo injection and that in vivo depletion of myeloid cells reduced the number of blood vessels formed at 7 days, indicating a positive, functional role for myeloid cells in building bio-engineered human blood vessels.

2. Steady improvement on cellular isolation, expansion and cryopreservation techniques for human EPCs and MPCs

3. Success with in vivo tracking of luciferase-labeled EPCs (Figure 1) in the liver regeneration model.

V. REPORTABLE OUTCOMES:

Manuscripts published April, 24, 2009-April 23, 2010:

Hjortnaes J, Gottlieb D, Figueiredo JL, Melero-Martin J, Kohler RH, Bischoff J, Weissleder R, Mayer J, Aikawa E. Intravital molecular imaging of small-diameter tissue-engineered vascular grafts: A feasibility study.Tissue Eng Part C Methods.2009 Sep 14. [Epub ahead of print] PMID: 19751103

Melero-Martin JM, De Obaldia ME, Allen P, Dudley AC, Klagsbrun M, Bischoff J. Host myeloid cells are necessary for creating bio-engineered human vascular networks in vivo.

Figure 1: Luciferase-labeled cbEPC and MPC localized to the liver/spleen region at Day 4.

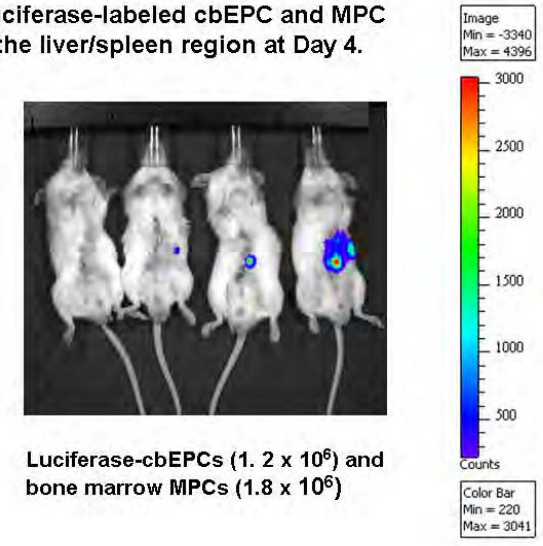

Luciferase-cbEPCs (1. 2 x 10^6) and bone marrow MPCs (1.8 x 10^6)

Tissue Eng Part A. 2010 Apr 20. [Epub ahead of print]PMID: 20218762
Awards:
**2009 Best Manuscript Award, Circulation Research, award received in November 2009 at the Circulation Research Editorial Board Meeting, Orlando FL for the following manuscript:

Melero-Martin JM, De Obaldia ME, Kang SY, Khan ZA, Yuan L, Oettgen P, Bischoff J. Engineering robust and functional vascular networks in vivo with human adult and cord blood-derived progenitor cells.
Circ Res. 2008; 103(2): 194-202

Invited Presentations related to this project given by Dr. Bischoff between April 24, 2009 - April 23, 2010

2009 Center for Vascular Remodeling and Regeneration, University of Pittsburgh, Pittsburgh, PA
May Keynote Speaker
Title: Building Blood Vessels with Human Blood- and Bone Marrow-derived Progenitor Cells

2009 International Stem Cell Meeting/ Israel Stem Cell Society, Tel Aviv Israel
June Invited Speaker/Plenary Session
Title: Tissue Vascularization using Blood- and Bone Marrow-derived Progenitor Cells

2009 Buck Institute for Age Research, Novato, CA
Oct Seminar Speaker
Title: Building Blood Vessels with Human Blood- and Bone Marrow-derived Progenitor Cells

2009 CardioVascular Institute, Beth Israel Deaconess Medical Center, Harvard Medical School, MA Dec Seminar Speaker
Title: Building Blood Vessels with Human Blood- and Bone Marrow-derived Progenitor Cells

2010 Wound Healing Society, Orlando, FL
April Plenary Session Speaker
Title: Building Blood Vessels with Human Blood- and Bone Marrow-derived Progenitor Cells

Upcoming Invited presentations related to this project:
2010 Eleventh International Workshop on Scleroderma Research
Boston University, Boston, MA August 1-4, 2010
Invited Speaker
2010 International Society for Applied Cardiovascular Biology
(ISACB), 12th Biennial Meeting, Boston, MA September 22-25, 2010
Invited Speaker

VI. CONCLUSIONS:

Our in vitro studies performed during this funding year have added practical, useful information concerning the culture and expansion of human EPCs and MPCs that will enhance the feasibility of using these cells for clinical application. Our in vivo studies (Objective 3) are encouraging in that we have an approach to test the ability of the EPCs and MPCs to assemble into functional vascular networks in regenerating liver. Moving from the Matrigel model to a tissue/organ model represents a critical step in this project and in eventual translation of this research to clinical application. We will seek new funding mechanisms, from the DOD or other funding agencies, to continue this work after the July 31, 2010 termination date.

"So what section"

Our goal is to build vascular networks from human endothelial progenitor cells (EPCs) and mesenchymal progenitor cells (MPCs) to re-build damaged tissues and organs. We have shown that human EPCs and MPCs can be obtained from blood or bone marrow and expanded in the laboratory without difficulty. Our published data demonstrate the vasculogenic capability of these cells in vivo. In the future, we envision use of a patient's own EPCs and MPCs for a variety of tissue-engineering (TE) and regenerative medicine applications. In summary, we envision our two-cell system as an *enabling technology* that can be applied to many different tissues/organs wherein functional blood vessels are needed.

VII. REFERENCES:

1. Melero-Martin JM, Khan ZA, Picard A, Wu X, Paruchuri S, Bischoff J. In vivo vasculogenic potential of human blood-derived endothelial progenitor cells. *Blood.* 2007;109(11):4761-4768.

2. Melero-Martin JM, De Obaldia ME, Kang SY, Khan ZA, Yuan L, Oettgen P, Bischoff J. Engineering robust and functional vascular networks in vivo with human adult and cord blood-derived progenitor cells. *Circ. Res.* 2008;103(2):194-202.

3. Melero-Martin JM, De Obaldia ME, Allen P, Dudley AC, Klagsbrun M, Bischoff J. Host Myeloid Cells Are Necessary for Creating Bioengineered Human Vascular Networks In Vivo. *Tissue Eng Part A.*

4. Reinisch A, Hofmann NA, Obenauf AC, Kashofer K, Rohde E, Schallmoser K, Flicker K, Lanzer G, Linkesch W, Speicher MR, Strunk D. Humanized large-scale expanded endothelial colony-forming cells function in vitro and in vivo. *Blood.* 2009;113(26):6716-6725.

5. Stroncek JD, Grant BS, Brown MA, Povsic TJ, Truskey GA, Reichert WM. Comparison of endothelial cell phenotypic markers of late-outgrowth endothelial progenitor cells isolated from patients with coronary artery disease and healthy volunteers. *Tissue Eng Part A.* 2009;15(11):3473-3486.

6. Alwayn IP, Verbesey JE, Kim S, Roy R, Arsenault DA, Greene AK, Novak K, Laforme A, Lee S, Moses MA, Puder M. A critical role for matrix metalloproteinases in liver regeneration. *J. Surg. Res.* 2008;145(2):192-198.

VIII. APPENDICES:

Pdfs for the following manuscripts:

Melero-Martin JM, De Obaldia ME, Allen P, Dudley AC, Klagsbrun M, **Bischoff J**. Host myeloid cells are necessary for creating bio-engineered human vascular networks in vivo. Tissue Eng Part A. 2010 Apr 20. [Epub ahead of print]PMID: 20218762

Hjortnaes J, Gottlieb D, Figueiredo JL, **Melero-Martin J**, Kohler RH, **Bischoff J**, Weissleder R, Mayer J, Aikawa E. Intravital molecular imaging of small-diameter tissue-engineered vascular grafts: A feasibility study. Tissue Eng Part C Methods. 2009 Sep 14. [Epub ahead of print] PMID: 1975

TISSUE ENGINEERING: Part A
Volume 00, Number 00, 2010

DOI: 10.1089/ten.tea.2010.0024

Original Article

Host Myeloid Cells Are Necessary for Creating Bioengineered Human Vascular Networks *In Vivo*

Juan M. Melero-Martin, Ph.D.,[1,2] Maria E. De Obaldia, A.B.,[1] Patrick Allen, B.S.,[1] Andrew C. Dudley, Ph.D.,[1] Michael Klagsbrun, Ph.D.,[1,3] and Joyce Bischoff, Ph.D.[1]

The recruitment of myeloid cells has been consistently associated with the formation of new blood vessels during pathological angiogenesis. However, the participation of myeloid cells in bioengineered vascular networks remains unclear. Therefore, we tested whether host myeloid cells play a role in the formation of bioengineered vascular networks that occurs *in vivo* upon coimplantation of blood-derived endothelial progenitor cells and bone-marrow-derived mesenchymal progenitor cells, suspended as single cells in Matrigel, into immune-deficient mice. We observed an influx of spatially organized host $CD11b^+$ myeloid cells into the Matrigel implant 1 to 3 days after implantation, which was shown to be cell mediated rather than a nonspecific response. Myeloid cells were significantly reduced once the implants were fully vascularized at days 6 and 7, suggesting an active role during steps that precede formation of functional anastomoses and perfused vessels. Importantly, depletion of circulating myeloid cells resulted in a significant reduction in microvessel density in the implants. In summary, the recruitment of myeloid cells occurs rapidly after coimplantation of endothelial and mesenchymal progenitor cells and is necessary for full vascularization in this model. This is the first demonstration of a role for recruited myeloid cells in the formation of bioengineered vascular networks.

Introduction

The participation of bone-marrow-derived mononuclear cells (MNCs) in pathological neovascularization has been well studied. For example, numerous clinical and experimental reports have shown that infiltrated accessory myeloid cells, including monocyte/macrophages, neutrophils, eosinophils, mast cells and dendritic cells, actively contribute to tumor progression by modulating angiogenesis.[1–6] Less well-studied is the role of myeloid cells in non-neoplastic neovascularization; however, experimental hind limb ischemia models suggest that the initiation of angiogenesis is related to a neutrophil-mediated increase in matrix metalloproteinases (MMP)-2 and -9 activity.[7] In other studies, subpopulations of myeloid cells were observed at the tips of nascent capillaries in neonatal murine retina[8] and in experimental models of growth factor-induced angiogenesis and tissue regeneration.[9–12] Taken together, these studies suggest that myeloid cells facilitate the comigration and the spatial arrangement of multiple cell types and assist progenitor cells during neovascularization in health and disease.

The pro-angiogenic features of subpopulations of peripheral blood MNCs have been recognized,[13,14] and even though their participation during neovascularization has led to some confusion over the definition of endothelial progenitor cells (EPCs), there is now a better consensus on the distinction between the accessory role of myeloid cells and the lumen forming, structural role of true EPCs.[15] Another example of the pro-angiogenic role is the apparent beneficial effect of autologous bone-marrow-derived MNCs administered to ischemic tissues,[16,17] findings that have prompted clinical trials.[18] Finally, myeloid cells have also been shown to influence neo-vessel formation by paracrine mechanisms when recruited to perivascular sites of neovascularization.[19]

We and others have proposed the combined use of EPCs and mesenchymal progenitor cells (MPCs) to engineer vascular networks *in vivo*.[20–22] Here we show for the first time that a population of recruited $CD11b^+$ myeloid cells constitutes an important cellular component of this vasculogenic process and that their recruitment should be considered a necessary step during the early events that take place after implantation of endothelial and mesenchymal progenitors.

Materials and Methods

In vivo *vasculogenesis assay*

EPC/MPC-driven vasculogenesis *in vivo* was evaluated using a previously described xenograft model.[21,23] Briefly, EPCs and MPCs (40:60 ratio; 1.9×10^6 cells total) were resuspended in 200 μL of Matrigel and injected subcutaneously

[1]Vascular Biology Program and Department of Surgery, Children's Hospital Boston, Harvard Medical School, Boston, Massachusetts.
Departments of [2]Cardiac Surgery and [3]Pathology, Children's Hospital Boston, Harvard Medical School, Boston, Massachusetts.

into 6-week-old male athymic nu/nu mice ($n = 4$ or $n = 5$, as indicated, for each experimental condition). (The immune-deficient nu/nu mice are lacking in B-cells.) The following implants served as controls: (a) Matrigel without cells, (b) Matrigel with EPCs alone, (c) Matrigel with MPCs alone, and (d) Matrigel with human MNCs (hMNCs; 3×10^6 in 200 μL of Matrigel). Additional controls were performed using mouse dermal endothelial cells and mouse bone-marrow-derived MPCs isolated from C57BL/6 mice[24] (40:60 ratio; 1.9×10^6 cells total) injected into either (a) 6-week-old male athymic nu/nu mouse or (b) 6-week-old male immune-competent C57BL/6 mice.

Myeloid depletion experiment

Rat Ly-6G (Gr-1) (herein referred to as Gr-1) or control (rat immunoglobulin G [IgG]2b) antibodies at 200 mg/mouse were administered intraperitoneally as follows: 2 days before Matrigel-EPC/MPC implantation, the same day of Matrigel implantation, and 3 days postimplantation. Each group was performed with five mice. Myeloid cell depletion was confirmed on blood samples by flow cytometry (FC) using Gr-1 antibody. Implants from each group were harvested at days 2 and 7 and analyzed by histology. Blood was withdrawn from the retro orbital sinus for complete blood count (CBC) with differential analyses (Department of Laboratory Medicine at Children's Hospital Boston).

Analysis

The presence of myeloid cells was evaluated by both FC and immunohistochemistry using antibodies against CD11b and Gr-1. EPCs were observed using a human-specific antibody against CD31 (hCD31). Evaluation of explant microvessel density (MVD) was carried out as described.[23,25]

Statistical analysis

The data were expressed as mean ± standard error of mean. Unless otherwise stated, all p-values reported were generated by two-tailed Student's unpaired t-tests. Additionally, multiple comparisons were performed where appropriate by one-way analysis of variance followed by Tukey's multiple comparison tests. p-Values <0.05 were considered statistically significant.

An Expanded Methods section (Supplemental Material, available online at www.liebertonline.com/ten) describes cell isolation and expansion, cell retrieval from Matrigel explants, FC, histology and immunohistochemistry, retroviral transduction, and MVD.

Results

Progressive vascularization of implants

We previously showed that coimplantation of EPCs and MPCs in Matrigel into immunodeficient mice leads to extensive networks of human blood vessels with functional anastomoses to the host circulatory system.[21] In particular, vascular networks contained erythrocytes by day 7 and implants remained vascularized for up to 4 weeks. We have now studied time points <7 days to analyze cellular events before the onset of connections between human and murine vessels. Human EPCs and MPCs were implanted, and explants examined at daily intervals ($n = 4$, each day) (Fig. 1). Gross examination at the time of harvest revealed partial vascularization of some implants (judged by the red color) at time points earlier than day 7 (Fig. 1A), suggesting that the formation of functional anastomoses occurs progressively during the first week. Histological analyses supported progressive appearance of functional blood vessels as shown by the presence of erythrocyte-filled vessels in hematoxylin and eosin (H&E)–stained sections and immunohistochemical staining of the lumenal structures with hCD31 antibody (Fig. 1B). Some implants showed partial vascularization at day 3 to 5. Specifically, one of four implants at day 3, two of four at day 4, and three of four at day 5 were vascularized. Finally, all implants were perfused at days 6 and 7. Quantification of the average MVD in implants that were vascularized (Fig. 1D) revealed a significant increase between day 5 (37 ± 11 vessels/mm^2, average ± standard deviation) and day 7 (97 ± 14 vessels/mm^2). These results suggested that from day 5 to 7, vascularization was still in progress.

Early presence of infiltrated host myeloid cells

Histological examination of the implants at daily intervals also revealed what appeared to be polymorphonuclear leukocytes at day 2 (red arrows in Fig. 1B). These cells were spatially organized into bundles of cells with some arranged into cellular cords and/or circular clusters. This observation suggested an involvement of host-derived leukocytes early in the vasculogenic process. To confirm the contribution of murine cells at different stages of vascularization, we implanted green fluorescent protein (GFP)–transfected MPCs together with unlabeled EPCs and examined the explants at daily intervals ($n = 4$, each day) (Fig. 2A). This combination of GFP-MPCs and EPCs allowed unequivocal tracking of both cell types by confocal microscopy. MPCs were identified as GFP positive (green staining in Fig. 2A), whereas EPCs were observed using a hCD31 followed by a Texas Red–conjugated secondary antibody (red staining in Fig. 2A). This analysis allowed for the identification of unstained nucleated murine cells that had infiltrated the implants (i.e., 4′,6-diamidino-2-phenylindole (DAPI$^+$), GFP$^-$, and hCD31$^-$ cells in Fig. 2A). Murine cells infiltrated as early as day 1 (Fig. 2A, left panel), with increased abundance at day 2 (middle panel), and a progressive decrease thereafter. Of note, at day 7, few murine cells remained, and as expected based on our previous work, EPCs and MPCs were found at lumenal and perivascular locations, respectively (Fig. 2A, right panel).

To confirm the presence of infiltrated murine leukocytes, we carried out flow cytometric analysis of the cells retrieved from the implants by enzymatic digestion at days 2 and 7. Using a murine-specific antibody against the pan-hematopoietic marker CD45 (see Supplemental Fig. S1, available online at www.liebertonline.com/ten for antibody specificity), we found that implants contained 34.2% murine CD45$^+$ (mCD45$^+$) cells at day 2. This number dropped to 6.1% by day 7 (Fig. 2B, C), confirming the histological observation of more murine cells present at the early time points. At the same time, the percentage of hCD31$^+$ cells (EPCs) increased from 44.7% (day 2) to 54.2% (day 7), whereas the percentage of hCD90$^+$ cells (MPCs) increased from 18.1% at day 2 to 36.7% at day 7 (Supplemental Fig. S2, available online at www.liebertonline.com/ten). These increases

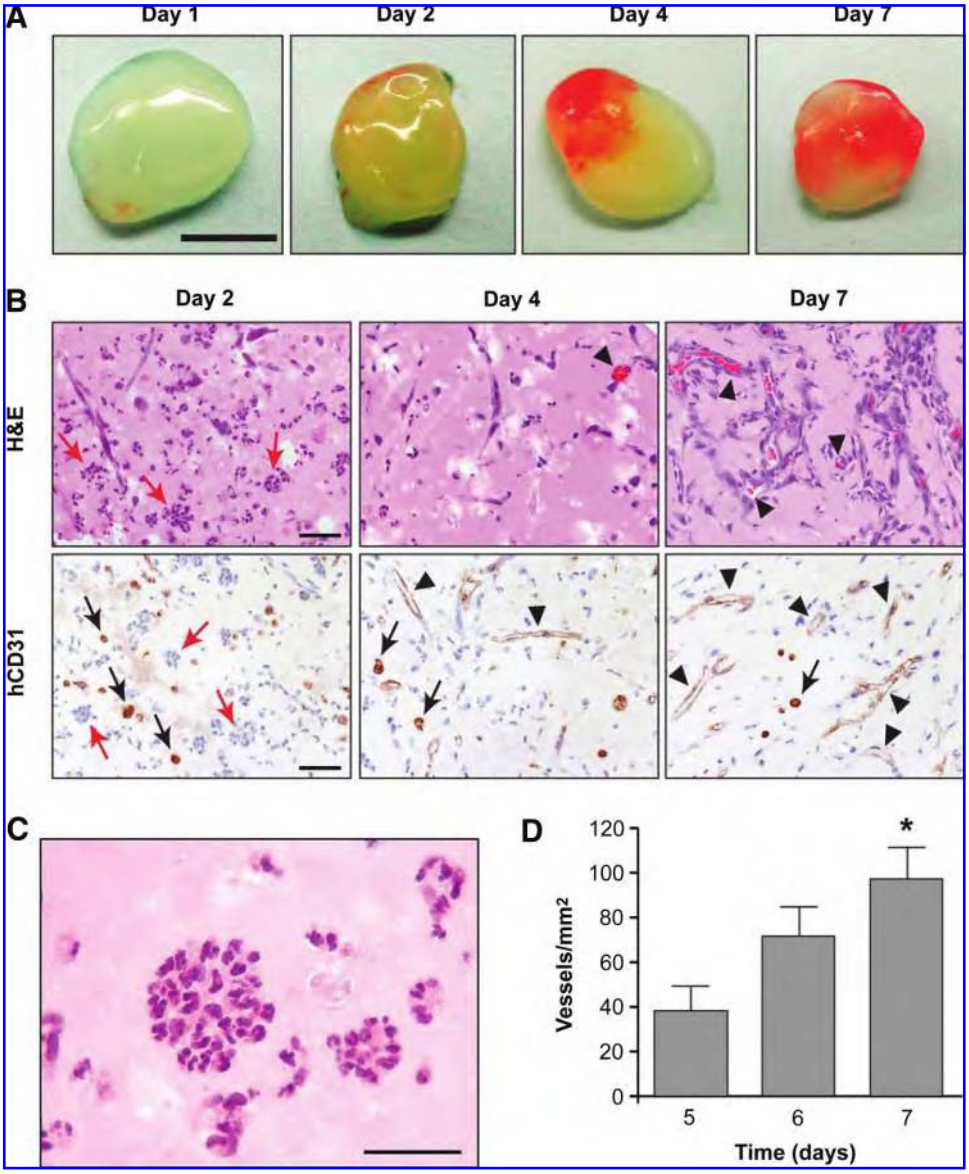

FIG. 1. Time course of bioengineered vascularization. EPCs/MPCs were implanted in nu/nu mice by subcutaneous injection and harvested at daily intervals ($n = 4$). (**A**) Macroscopic view of explanted Matrigel (scale bar, 500 μm). (**B**) H&E and hCD31 immunohistochemical staining of explants harvested at days 2, 4, and 7. The presence of blood vessels containing erythrocytes was evident from day 4 (black arrowheads). Both microvessels and individual EPCs (black arrows) stained positive for hCD31. In addition, day 2 explants contained circular clusters of polymorphonuclear cells (red arrows). Scale bar, 50 μm. (**C**) High-power image of implant removed at day 2 to show morphology of circular clusters (scale bar, 30 μm). (**D**) Microvessel density quantification was performed by counting erythrocyte-filled vessels in all implants. Each bar represents the mean ± standard deviation (vessels/mm^2) obtained from only vascularized implants. *$p < 0.05$ compared to implants harvested at day 5. EPCs, endothelial progenitor cells; MPCs, mesenchymal progenitor cells; H&E, hematoxylin and eosin; hCD31, human-specific antibody against CD31. Color images available online at www.liebertonline.com/ten.

in the percentages of EPCs and MPCs at day 7 are in part explained by the less prominent presence of murine hematopoietic cells.

To specifically examine the presence of myeloid cells we used an antibody against mCD11b. Myeloid lineage cells, including monocytes, polymorphonucleated granulocytes (i.e., neutrophils, eosinophils, and basophils), and mast cells,[1] express CD11b in addition to CD45. In contrast, lymphocytes (the other major nucleated cell population) are negative for CD11b, with the exception of natural killer cells. Since all CD11b$^+$ myeloid cells are also CD45$^+$, we quantified the CD11b$^+$/CD45$^+$ cell ratio in the implants and compared it to the ratio found in the peripheral blood of the implant-bearing mice (Fig. 2B, D) at day 2. The peripheral blood ratio was 58.2%. In contrast, the implant ratio was 98.1%, indicating that myeloid cells preferentially migrated into the implants during the early days of the vasculogenic process. Immunostaining with an antibody against CD11b (see Supplemental Fig. S3, available online at www.liebertonline.com/ten for controls) supported the observation that infiltrated

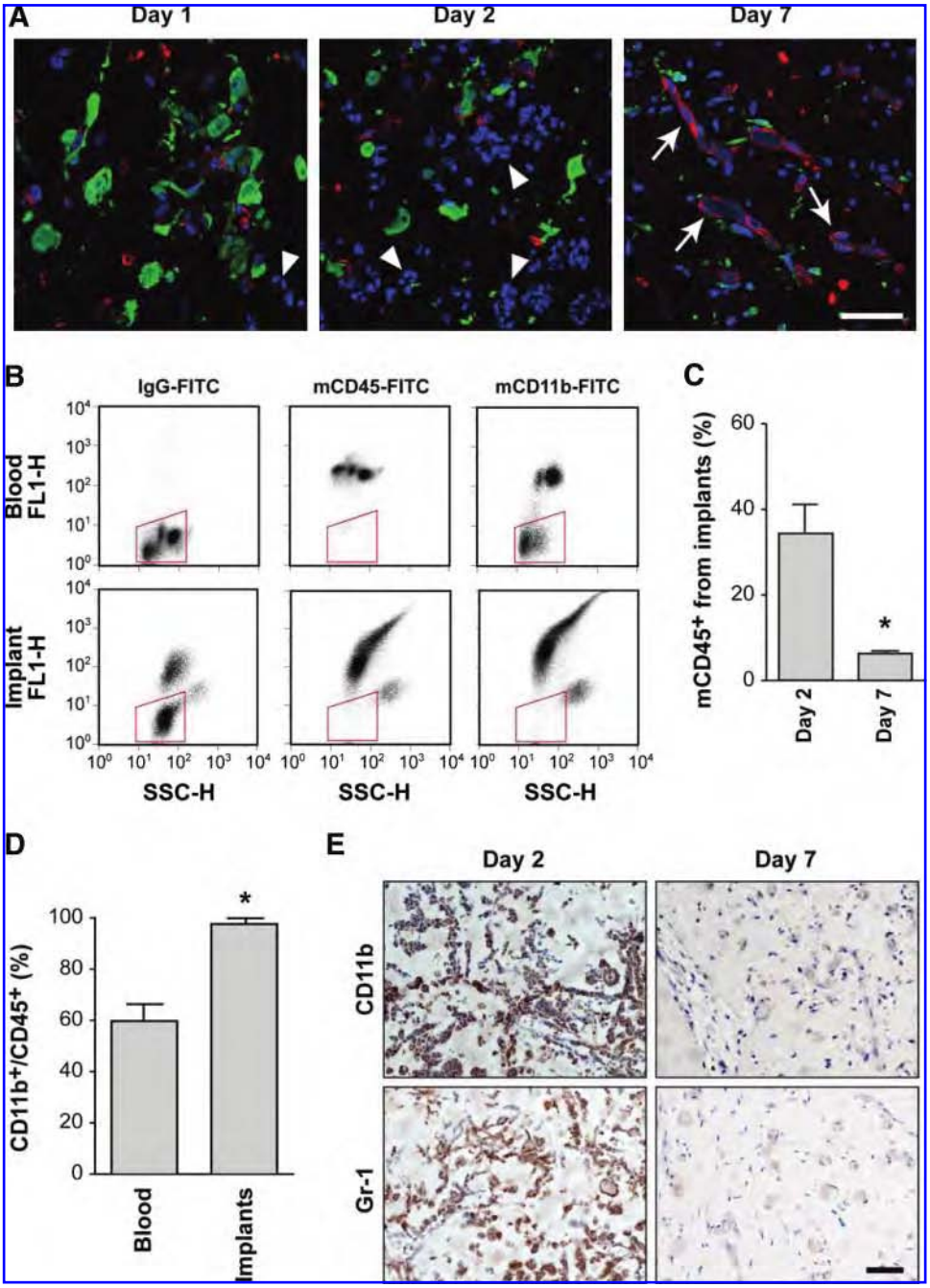

FIG. 2. Early infiltration of host myeloid cells. Matrigel implants containing EPCs and either GFP-MPCs (**A**) or unlabeled MPCs (**B–E**). (**A**) Confocal microscopy of immunostained sections from implants harvested at different time points (green, red, and blue staining correspond to GFP, hCD31, and DAPI, respectively). Host cells ($DAPI^+$, GFP^-, $hCD31^-$; white arrowheads) were first seen at day 1 (left panel), were abundant at day 2 (middle panel), and declined thereafter. Perfused human vessels (white arrows) were observed at day 7 with EPCs (red) and MPCs (green) found at lumenal and perivascular locations, respectively (right panel). Scale bar, 50 μm. (**B, C**) Flow cytometry analysis of cells obtained from both implants and peripheral blood were carried out at days 2 and 7 ($n = 4$ at each time point) with antibodies against mCD45 and mCD11b. Representative dot-plot diagrams from day 2 are depicted. Red box shows region of nonstained hematopoietic cells. (**C**) Quantitative analyses showed that the number of infiltrated $mCD45^+$ cells at day 2 was significantly higher than at day 7 ($^*p < 0.05$, $n = 4$). (**D**) Quantitative analyses at day 2 revealed that the ratio $CD11b^+/CD45^+$ cells in the implants was significantly higher than in peripheral blood ($^*p < 0.05$, $n = 4$). (**E**) The presence and absence of myeloid cells at days 2 and 7, respectively, were confirmed using antibodies against CD11b and Gr-1. Images at each time point are representative of implants harvested from four different mice (scale bars, 50 μm). GFP, green fluorescent protein; mCD45, murine CD45; IgG, immunoglobulin G; FITC, fluorescein isothiocyanate. DAPI, 4′,6-diamidino-2-phenylindole; FL1-H, fluorescence channel-1 for FITC; SSC-H, side light scatter. Color images available online at www.liebertonline.com/ten.

$CD11b^+$ cells were abundant at day 2 but barely detectable at day 7 (Fig. 2E). In fact, the low detection of $CD11b^+$ cells throughout the tissue at day 7 suggested that the number of $CD11b^+$ found by FC (Fig. 2C) likely corresponded to myeloid cells present in the peripheral blood in the implant vessels. Similar results were found using an antibody against Gr-1, a marker shared by granulocytes and some monocytes.[1] Infiltrated $Gr\text{-}1^+$ cells were abundant at day 2 but less so at day 7 once the implants became fully vascularized (Fig. 2E).

To elucidate the cellular components of the implant responsible for the early infiltration of murine myeloid cells, we compared the following ($n = 4$ for each group): (a) our standard EPCs/MPCs in Matrigel, (b) Matrigel without cells, (c) EPCs alone in Matrigel, (d) MPCs alone in Matrigel, and (e) hMNC alone in Matrigel. Histological and anti-CD11b staining of the explants at day 2 revealed that both EPCs and MPCs alone were able to instigate the recruitment of myeloid cells (Fig. 3). In contrast, implants with Matrigel alone showed minimal cell infiltration, suggesting that Matrigel itself was inert and the presence of infiltrated myeloid cells was cell mediated. Medium components such as fetal bovine serum in the implant did not cause myeloid cell recruitment, since Matrigel implants spiked with culture medium also lacked murine cell infiltration (data not shown). To elucidate whether the recruitment of myeloid cells was due to the fact that our model uses human cells, hMNCs in Matrigel were tested, but showed no signs of $CD11b^+$ murine cell infiltration by immunostaining (Fig. 3) or by FC (not shown). Thus, the lack of $mCD11b^+$ cells indicated specificity; human cells *per se* were not sufficient to instigate the recruitment of host myeloid cells into Matrigel. In another test, we substituted human EPCs and MPCs with murine dermal endothelial cells and murine MPCs, both cell types isolated from C57BL/6 mice,[24] and implanted into either nu/nu mice (Fig. 3 bottom panels) or into immune-competent C57BL/6 mice ($n = 4$ each group; see Supplemental Fig. S4, available online at www.liebertonline.com/ten). At day 2, implants from both groups of mice presented a large number of infiltrated myeloid cells as observed by H&E and CD11b staining, again indicating that recruitment was not due to a reaction against human cells, or a consequence of using immune-deficient mice as an animal model.

MMP-9 and -2 expression by infiltrated murine myeloid cells

The infiltration of myeloid cells at sites of neovascularization has been associated with expression of MMPs. To investigate whether the infiltrated myeloid cells expressed MMP-9 and -2, we carried out double-label immunofluorescence (CD11b/MMP-9 and CD11b/MMP-2) on sections taken from explants at days 2 and 7. As depicted in Figure 4, $CD11b^+$ cells expressing MMP-9 were very abundant at day 2, but negligible at day 7 (the fluorescent signal detected within the lumen of multiple blood vessels at day 7 was an artifact caused by erythrocyte autofluorescence). Expression of MMP-2 by some infiltrated $CD11b^+$ cells was also evident at day 2, although MMP-9-expressing cells appeared to predominate. Expression of both CD11b and MMP-2 at day 7 was absent, suggesting the absence of infiltrated myeloid cells at later stages of the vasculogenic process. Control

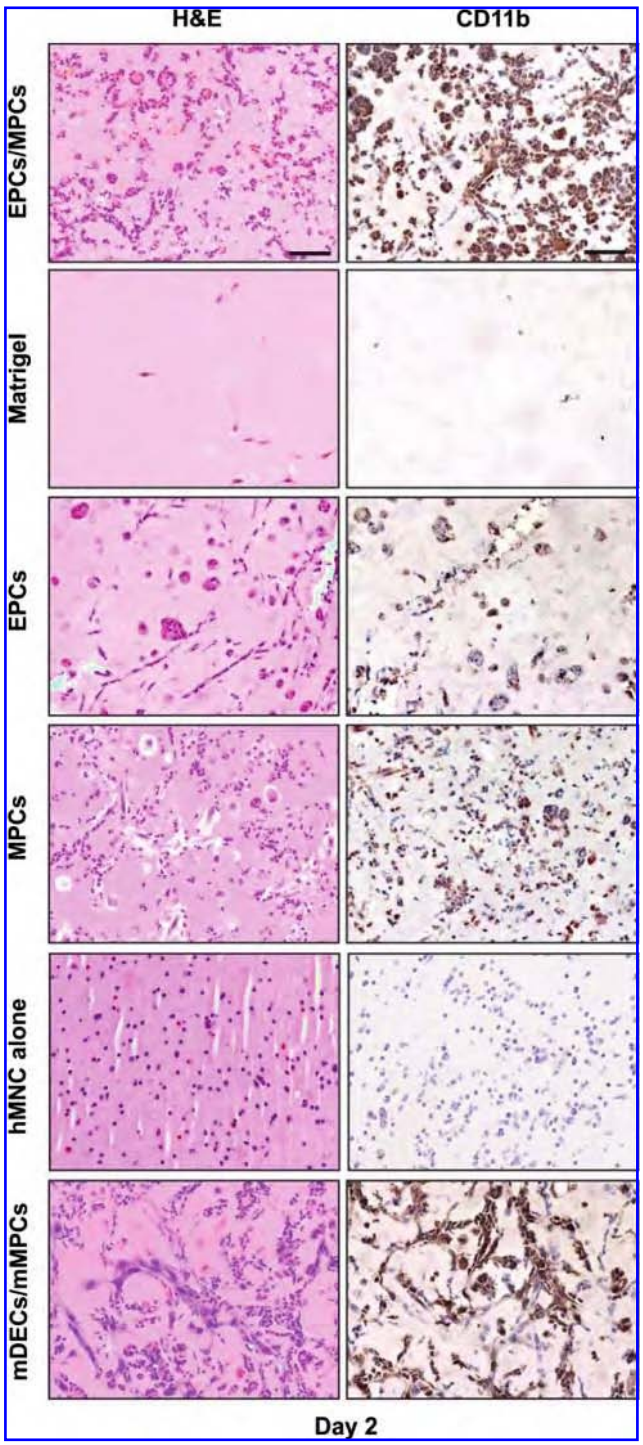

FIG. 3. Cell-mediated infiltration of $CD11b^+$ cells. Matrigel implants containing either EPCs and MPCs, no cells, EPCs alone, MPCs alone, human MNCs alone, or mDECs and mMPCs. Implants were harvested at day 2 ($n = 4$) and stained by H&E (left column) and CD11b immunohistochemistry (right column). Images are representative of explants harvested from four different mice (scale bars, 50 μm). MNCs, mononuclear cells; mDECs, mouse dermal endothelial cells; mMPCs, mouse bone-marrow-derived mesenchymal progenitor cells. Color images available online at www.liebertonline.com/ten.

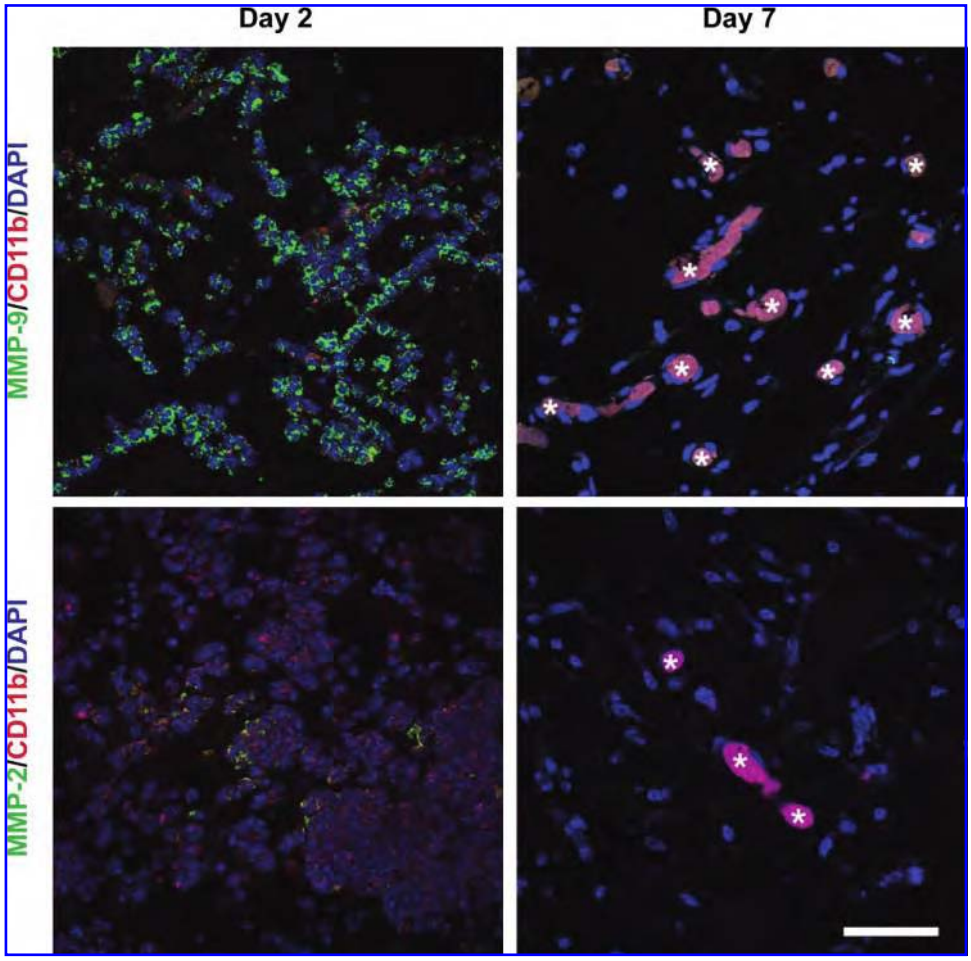

FIG. 4. MMP-9 and -2 expression by infiltrated myeloid cells. Matrigel implants containing EPCs and MPCs were harvested at day 2 (left column) and day 7 (right column). Double immunofluorescent staining was carried out using antibodies against MMP-9 (green) and CD11b (red) or MMP-2 (green) and CD11b (red) (top and bottom panels, respectively). Confocal microscopy revealed abundant $CD11b^+$ cells expressing MMP-9 at day 2, and negligible expression at day 7. Expression of MMP-2 by some infiltrated $CD11b^+$ cells was also evident at day 2, but absent at day 7. The fluorescent signal detected within lumens at day 7 was due to erythrocyte autofluorescence (asterisks). Images at each time point are representative of implants harvested from four different mice (scale bars, 50 μm). MMP, matrix metalloproteinase. Color images available online at www.liebertonline.com/ten.

staining for MMP-9 and -2 expression was carried out with sections from mouse liver and spleen (Supplemental Fig. S5, available online at www.liebertonline.com/ten).

Depletion of circulating myeloid cells impairs vasculogenesis

To elucidate whether the infiltrated myeloid cells are necessary during the vascularization process, we implemented a strategy that has proved effective in the depletion of circulating $Gr\text{-}1^+$ cells from the peripheral blood of mice.[26] Two groups of mice ($n = 5$ each) were given, by intraperitoneal injection, 200 mg/mouse of either anti-Gr-1 or IgG control antibodies 2 days before, the day of, and 3 days after EPCs/MPCs implantation (Fig. 5A). The successful depletion of $Gr\text{-}1^+$ cells from the mouse peripheral blood is shown in Figure 5B by FC analysis: IgG-treated mice presented 57.3% $Gr\text{-}1^+$ cells at day 2, whereas the αGr-1-treated group had only 7.9%. Myeloid depletion was also evident from the CBC with differential analyses of the blood from each group of mice. The CBC showed a significantly reduced level of both neutrophils and monocytes in the αGr-1-treated group (see full analysis in Supplemental Fig. S6, available online at www.liebertonline.com/ten). Depletion of circulating myeloid cells affected the number of infiltrated $CD11b^+$ cells seen in the implants. As expected, both H&E- and CD11b-stained sections of explants harvested at day 2 from the IgG-treated mice showed abundant and uniform presence of infiltrated myeloid cells (Fig. 5C). In contrast, the number of infiltrated CD11b cells in the αGr-1-treated group was significantly reduced and their presence was limited to the periphery of the implants, suggesting that remaining circulating myeloid cells were insufficient to infiltrate the implant. This pattern of impaired myeloid cell recruitment correlated with expression of MMP-9 as observed by immunofluorescent staining: IgG-treated mice showed uniform expression of MMP-9, whereas implants from αGr-1-treated mice showed MMP-9 limited to the periphery (Fig. 5D, E).

We then evaluated the effect of myeloid cell depletion on the formation of blood vessels at day 7. As expected, systemic treatment with IgG had no detrimental effect on the formation of vascular networks. A large number of human-specific lumenal structures containing erythrocytes were observed in H&E- and hCD31-stained sections; however, explants taken from the αGr-1-treated mice showed a reduction in the number of blood vessels (Fig. 6). MVD quantification revealed a statistically significant ($p = 0.01$) reduction of 52.8% in the number of blood vessels found in the αGr-1-treated mice ($33 + 8$ vessels/mm^2) as compared to the IgG-treated mice ($71 + 9$ vessels/mm^2), indicating that depletion of circulating myeloid cells impaired the process of vasculogenesis.

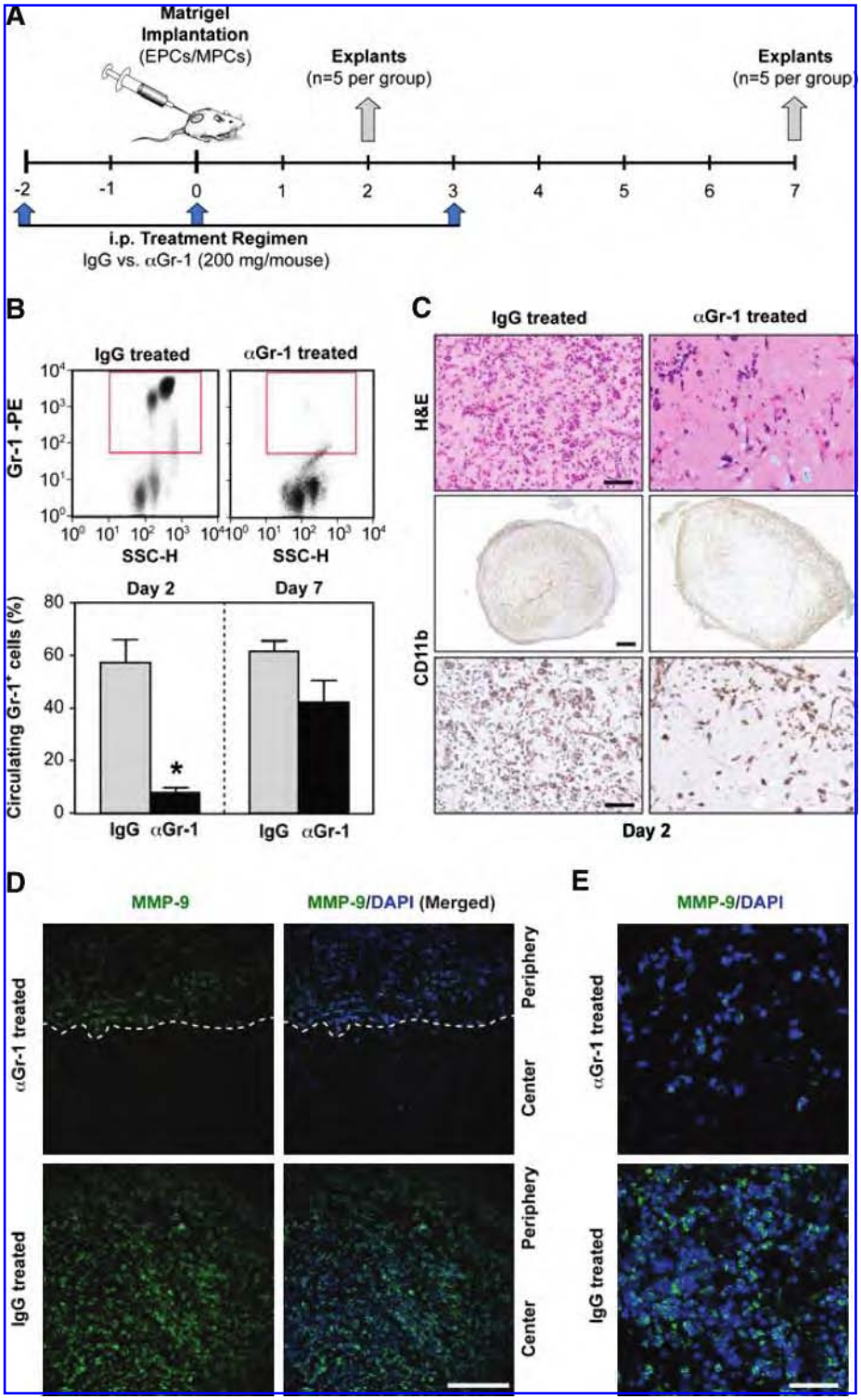

FIG. 5. Systemic depletion of circulating myeloid cells. (**A**) Two groups of mice received 200 mg/mouse of either anti Gr-1 (αGr-1 treated) or control IgG (IgG treated) antibodies by intraperitoneal injection at three time points as shown. Matrigel implants containing EPCs and MPCs were injected subcutaneously and harvested at days 2 and 7 ($n = 5$). (**B**) Flow cytometry analyses of peripheral blood MNCs from implant-bearing mice were carried out with anti-Gr-1 to confirm myeloid depletion. Representative dot-plot diagrams from day 2 analyses are depicted. Red boxes indicate region of Gr-1-positive cells. Quantitative cytometric analyses from both groups of mice ($n = 5$) were compared at days 2 and 7 ($^*p < 0.05$; $n = 5$). (**C**) H&E and CD11b immunostaining carried out at day 2 showed a reduced number of infiltrated $CD11b^+$ cells in the αGr-1-treated group compared to IgG-treated mice (scale bars, 50 μm). (**D, E**) Immunostaining carried out at day 2 showed that infiltrated $MMP\text{-}9^+$ cells were reduced and preferentially located in the periphery of the implants in the αGr-1-treated group; in contrast, $MMP\text{-}9^+$ cells were abundant and uniformly distributed in implants from IgG-treated mice (**E:** scale bars, 200 μm; **D:** scale bar, 50 μm). **D:** White dashed line indicates demarcation between the center and periphery of the Matrigel implant. All images are representative of implants harvested from five different mice. Color images available online at www.liebertonline.com/ten.

Discussion

Since EPCs were first identified in peripheral blood,[27] there has been great motivation to apply these cells to new therapies for vascularization. Recently, we and other authors have proposed the combined use of EPCs and perivascular cells to engineer vascular networks *in vivo*,[20–22] but none of these studies investigated the participation of host cells as the nascent vessels form.

Using our vasculogenic model of subcutaneous coimplantation of human EPCs and MPCs into immune-deficient mice, we examined the contribution of host cells from the time of subcutaneous injection to the time at which blood vessels were fully formed. As expected, the formation of functional anastomoses was found to be progressive: perfused blood vessels were seen in the implants as early as day 3 (partial) with full vascularization achieved by day 7.[21] These results were similar to those reported by other authors using different perivascular cells[20,22]; however, it was the examination of early time points, before the appearance of perfused vessels, that revealed an abundant and unexpected presence of infiltrated murine myeloid ($CD45^+$, $CD11b^+$, $Gr\text{-}1^+$) cells. The myeloid cells were spatially organized in bundles and arranged into cellular cords and/or circular clusters. Two important aspects of our initial observations are the following: (1) the proportion of $CD11b^+/CD45^+$ was significantly higher in the implants (98%) than in peripheral blood (57%), suggesting recruitment of myeloid cells rather than a nonspecific diffusion of total white blood cells from potentially leaky vasculature, and (2) the presence of infiltrated myeloid cells was temporary; their disappearance coincided with the onset of anastomoses formation.

Even though myeloid cells have frequently been observed at sites of neovascularization, their presence often provokes debate about possible nonspecific inflammatory reactions. In this regard, we have demonstrated that the recruitment of host hematopoietic cells was specific and cell mediated based on the following observations: (1) both EPCs and MPCs, independently and in combination, were able to recruit $mCD11b^+$ cells to the Matrigel implant; (2) there was no such recruitment when Matrigel alone (with and without culture medium) was injected or when hMNCs were implanted; (3) murine endothelial and mesenchymal cells produced recruitment of myeloid cells similar to the human counterparts, ruling out the possibility of an inflammatory reaction driven by species differences. Past studies have shown that the role of recruited myeloid cells at sites of neovascularization is often multifaceted, and their presence has been associated with the production of vast array of pro-angiogenic cytokines and vascular-modulating enzymes, including MMPs.[1,3,28,29] In this context, we found that the large majority of infiltrated $CD11b^+$ cells uniformly expressed MMP-9, and to a lesser extent MMP-2. The potential for MMP-mediated matrix remodeling may in part explain the necessity of early host cellular support. Collectively, these observations suggest a purposeful recruitment of host circulating $CD11b^+$ cells by the implanted vasculogenic cells. Further work is needed to elucidate the molecular mechanism by which myeloid cells are recruited during the early steps of bioengineered vasculogenesis.

The definitive confirmation of active myeloid cell participation was found by carrying out depletion experiments. By significantly reducing the number of circulating myeloid cells available in the peripheral blood, implants recruited fewer $CD11b^+$ cells. Importantly, this reduction in myeloid cells correlated with a significant decrease in the number of perfused blood vessels found at day 7 (53% reduction in implants from myeloid-depleted mice). This finding clearly indicated an active and necessary involvement of host myeloid cells since their absence led to impaired (or at least delayed) vasculogenesis. In previous work, we showed that optimal vasculogenesis occurs when EPCs are combined with an appropriate source and proportion of perivascular cells (e.g., MPCs), and that neither cell type alone can produce high MVDs in Matrigel.[21] We have now found that both cell types are capable of host myeloid cell recruitment and this recruitment is necessary, but not sufficient to achieve rapid neovascularization at high density.

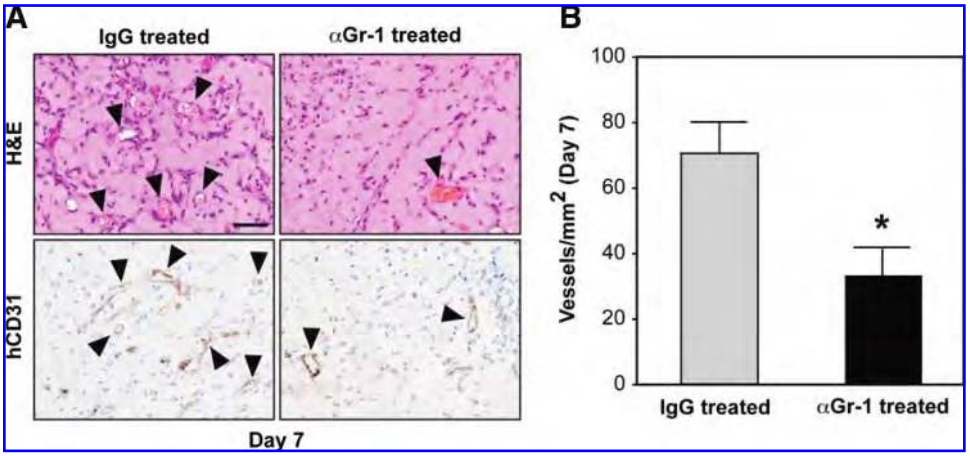

FIG. 6. Effect of myeloid cell depletion on posttransplantation vascularization. (**A**) Implants harvested at day 7 from both αGr-1- and IgG-treated mice. H&E and hCD31 immunohistochemistry revealed a reduced number of blood vessels (arrowheads) in the αGr-1-treated group. Images are representative of implants harvested from five different mice (scale bar, 50 μm). (**B**) Microvessel density quantification of αGr-1-treated mice as compared to the IgG-treated animals. Each bar represents the mean ± standard deviation (vessels/mm^2) (*$p < 0.05$; $n = 5$). Color images available online at www.liebertonline.com/ten.

In summary, we demonstrate for the first time that a population of recruited $CD11b^+$ myeloid cells plays an active role in the formation of bioengineered vascular networks using EPC and MPC. Myeloid cells were found to be increased at early time points, but their number was reduced when functional anastomoses between the newly formed lumens and the host circulation formed. Depletion of myeloid cells from peripheral blood before implantation resulted in a reduced number of blood vessels, indicating that the presence of myeloid cells is a necessary step during the early stages of vasculogenesis.

Acknowledgments

We would like to thank Dr. Dipak Panigrahy for advice with myeloid cell depletion experiments, Dr. Soo-Young Kang for assistance with retroviral transfections, Dr. Harry Kozakewich, Department of Pathology, Children's Hospital Boston, for initially helping us to identify the infiltrating cells, Jill Wylie-Sears for technical assistance, and Kristin Johnson for figure preparation. This research was supported by the Specialized Histopathology Services, Longwood Facility of the Dana-Farber/Harvard Cancer Center (P30 CA06516). This work was supported by the U.S. Army Medical Research and Materiel Command (W81XWH-05-1-0115).

Disclosure Statement

No competing financial interests exist.

References

1. Murdoch, C., Muthana, M., Coffelt, S.B., and Lewis, C.E. The role of myeloid cells in the promotion of tumour angiogenesis. Nat Rev Cancer **8,** 618, 2008.
2. Balkwill, F., Charles, K.A., and Mantovani, A. Smoldering and polarized inflammation in the initiation and promotion of malignant disease. Cancer Cell **7,** 211, 2005.
3. Coussens, L.M., and Werb, Z. Inflammation and cancer. Nature **420,** 860, 2002.
4. Pollard, J.W. Tumour-educated macrophages promote tumour progression and metastasis. Nat Rev Cancer **4,** 71, 2004.
5. Balkwill, F., and Mantovani, A. Inflammation and cancer: back to Virchow? Lancet **357,** 539, 2001.
6. De Palma, M., Venneri, M.A., Galli, R., Sergi Sergi, L., Politi, L.S., Sampaolesi, M., and Naldini, L. Tie2 identifies a hematopoietic lineage of proangiogenic monocytes required for tumor vessel formation and a mesenchymal population of pericyte progenitors. Cancer Cell **8,** 211, 2005.
7. Muhs, B., Gagne, P., Plitas, G., Shaw, J., and Shamamian, P. Experimental hindlimb ischemia leads to neutrophil-mediated increases in gastrocnemius MMP-2 and-9 …. J Surg Res **117,** 249, 2004.
8. Naug, H.L., Browning, J., Gole, G.A., and Gobe, G. Vitreal macrophages express vascular endothelial growth factor in oxygen-induced retinopathy. Clin Exp Ophthalmol **28,** 48, 2000.
9. Anghelina, M., Krishnan, P., Moldovan, L., and Moldovan, N.I. Monocytes and macrophages form branched cell columns in Matrigel: implications for a role in neovascularization. Stem Cells Dev **13,** 665, 2004.
10. Tigges, U., Hyer, E.G., Scharf, J., and Stallcup, W.B. FGF2-dependent neovascularization of subcutaneous Matrigel plugs is initiated by bone marrow-derived pericytes and macrophages. Development **135,** 523, 2008.
11. Anghelina, M., Krishnan, P., Moldovan, L., and Moldovan, N.I. Monocytes/macrophages cooperate with progenitor cells during neovascularization and tissue repair: conversion of cell columns into fibrovascular bundles. Am J Pathol **168,** 529, 2006.
12. Schmeisser, A., Garlichs, C.D., Zhang, H., Eskafi, S., Graffy, C., Ludwig, J., Strasser, R.H., and Daniel, W.G. Monocytes coexpress endothelial and macrophagocytic lineage markers and form cord-like structures in Matrigel under angiogenic conditions. Cardiovasc Res **49,** 671, 2001.
13. Gulati, R., Jevremovic, D., Peterson, T.E., Chatterjee, S., Shah, V., Vile, R.G., and Simari, R.D. Diverse origin and function of cells with endothelial phenotype obtained from adult human blood. Circ Res **93,** 1023, 2003.
14. Rehman, J., Li, J., Orschell, C.M., and March, K.L. Peripheral blood "endothelial progenitor cells" are derived from monocyte/macrophages and secrete angiogenic growth factors. Circulation **107,** 1164, 2003.
15. Yoder, M.C., Mead, L.E., Prater, D., Krier, T.R., Mroueh, K.N., Li, F., Krasich, R., Temm, C.J., Prchal, J.T., and Ingram, D.A. Redefining endothelial progenitor cells via clonal analysis and hematopoietic stem/progenitor cell principals. Blood **109,** 1801, 2007.
16. Kalka, C., Masuda, H., Takahashi, T., Kalka-Moll, W.M., Silver, M., Kearney, M., Li, T., Isner, J.M., and Asahara, T. Transplantation of *ex vivo* expanded endothelial progenitor cells for therapeutic neovascularization. Proc Natl Acad Sci U S A **97,** 3422, 2000.
17. Kocher, A.A., Schuster, M.D., Szabolcs, M.J., Takuma, S., Burkhoff, D., Wang, J., Homma, S., Edwards, N.M., and Itescu, S. Neovascularization of ischemic myocardium by human bone-marrow-derived angioblasts prevents cardiomyocyte apoptosis, reduces remodeling and improves cardiac function. Nat Med **7,** 430, 2001.
18. Schachinger, V., Assmus, B., Britten, M.B., Honold, J., Lehmann, R., Teupe, C., Abolmaali, N.D., Vogl, T.J., Hofmann, W.K., Martin, H., Dimmeler, S., and Zeiher, A.M. Transplantation of progenitor cells and regeneration enhancement in acute myocardial infarction: final one-year results of the TOPCARE-AMI Trial. J Am Coll Cardiol **44,** 1690, 2004.
19. Grunewald, M., Avraham, I., Dor, Y., Bachar-Lustig, E., Itin, A., Jung, S., Chimenti, S., Landsman, L., Abramovitch, R., and Keshet, E. VEGF-induced adult neovascularization: recruitment, retention, and role of accessory cells. Cell **124,** 175, 2006.
20. Traktuev, D.O., Prater, D.N., Merfeld-Clauss, S., Sanjeevaiah, A.R., Saadatzadeh, M.R., Murphy, M., Johnstone, B.H., Ingram, D.A., and March, K.L. Robust functional vascular network formation *in vivo* by cooperation of adipose progenitor and endothelial cells. Circ Res **104,** 1410, 2009.
21. Melero-Martin, J., De Obaldia, M.E., Kang, S.Y., Khan, Z.A., Yuan, L., Oettgen, P., and Bischoff, J. Engineering robust and functional vascular networks *in vivo* with human adult and cord blood-derived progenitor cells. Circ Res **103,** 194, 2008.
22. Au, P., Daheron, L., Duda, D.G., Cohen, K.S., Tyrrell, J.A., Lanning, R.M., Fukumura, D., Scadden, D.T., and Jain, R.K. Differential *in vivo* potential of endothelial progenitor cells from human umbilical cord blood and adult peripheral blood to form functional long-lasting vessels. Blood **111,** 1302, 2008.
23. Melero-Martin, J., and Bischoff, J. Chapter 13. An *in vivo* experimental model for postnatal vasculogenesis. Methods Enzymol **445,** 303, 2008.

24. Dudley, A.C., Khan, Z.A., Shih, S.C., Kang, S.Y., Zwaans, B.M., Bischoff, J., and Klagsbrun, M. Calcification of multipotent prostate tumor endothelium. Cancer Cell **14,** 201, 2008.
25. Melero-Martin, J., Khan, Z.A., Picard, A., Wu, X., Paruchuri, S., and Bischoff, J. *In vivo* vasculogenic potential of human blood-derived endothelial progenitor cells. Blood **109,** 4761, 2007.
26. Kaipainen, A., Kieran, M., Huang, S., Butterfield, C., Bielenberg, D., Mostoslavsky, G., Mulligan, R., Folkman, J., and Panigrahy, D. PPARalpha deficiency in inflammatory cells suppresses tumor growth. PLoS ONE **2,** e260, 2007.
27. Asahara, T., Murohara, T., Sullivan, A., Silver, M., van der Zee, R., Li, T., Witzenbichler, B., Schatteman, G., and Isner, J.M. Isolation of putative progenitor endothelial cells for angiogenesis. Science **275,** 964, 1997.
28. Coussens, L.M., Tinkle, C.L., Hanahan, D., and Werb, Z. MMP-9 supplied by bone marrow-derived cells contributes to skin carcinogenesis. Cell **103,** 481, 2000.
29. Coussens, L.M., Raymond, W.W., Bergers, G., Laig-Webster, M., Behrendtsen, O., Werb, Z., Caughey, G.H., and Hanahan, D. Inflammatory mast cells up-regulate angiogenesis during squamous epithelial carcinogenesis. Genes Dev **13,** 1382, 1999.

Address correspondence to:
Joyce Bischoff, Ph.D.
Vascular Biology Program and Department of Surgery
Children's Hospital Boston
Harvard Medical School
300 Longwood Ave.
Boston, MA 02115

E-mail: joyce.bischoff@childrens.harvard.edu

Received: January 15, 2010
Accepted: March 5, 2010
Online Publication Date: April 9, 2010

TISSUE ENGINEERING: Part C
Volume 00, Number 00, 2009

DOI: 10.1089/ten.tec.2009.0466

Methods Article

Intravital Molecular Imaging of Small-Diameter Tissue-Engineered Vascular Grafts in Mice: A Feasibility Study

Jesper Hjortnaes, B.Sc.,[1,*] Danielle Gottlieb, M.D.,[2,*] Jose-Luiz Figueiredo, M.D.,[1] Juan Melero-Martin, Ph.D.,[2] Rainer H. Kohler, Ph.D.,[1] Joyce Bischoff, Ph.D.,[2] Ralph Weissleder, M.D., Ph.D.,[1] John E. Mayer, M.D.,[2] and Elena Aikawa, M.D., Ph.D.[1]

Objectives: Creating functional small-diameter tissue-engineered blood vessels has not been successful to date. Moreover, the processes underlying the *in vivo* remodeling of these grafts and the fate of cells seeded onto scaffolds remain unclear. Here we addressed these unmet scientific needs by using intravital molecular imaging to monitor the development of tissue-engineered vascular grafts (TEVG) implanted in mouse carotid artery.
Methods and Results: Green fluorescent protein–labeled human bone marrow–derived mesenchymal stem cells and cord blood–derived endothelial progenitor cells were seeded on polyglycolic acid–poly-L-lactic acid scaffolds to construct small-caliber TEVG that were subsequently implanted in the carotid artery position of nude mice ($n = 9$). Mice were injected with near-infrared agents and imaged using intravital fluorescence microscope at 0, 7, and 35 days to validate *in vivo* the TEVG remodeling capability (Prosense680; VisEn, Woburn, MA) and patency (Angiosense750; VisEn). Imaging coregistered strong proteolytic activity and blood flow through anastomoses at both 7 and 35 days postimplantation. In addition, image analyses showed green fluorescent protein signal produced from mesenchymal stem cell up to 35 days postimplantation. Comprehensive correlative histopathological analyses corroborated intravital imaging findings.
Conclusions: Multispectral imaging offers simultaneous characterization of *in vivo* remodeling enzyme activity, functionality, and cell fate of viable small-caliber TEVG.

Introduction

An estimated 80,000 patients per year in the United States alone are not able to undergo coronary artery bypass grafting due to lack of suitable autologous vessels and poor function of currently available small-diameter synthetic vascular grafts.[1] Current synthetic grafts, made of nondegradable synthetic materials, have been used as vascular conduits in cardiovascular surgery. However, the small-caliber grafts have shown shortcomings, including thrombus formation resulting in poor patency rates, infection, and lack of growth and remodeling potential.[2] Small-caliber tissue-engineered vascular grafts (TEVGs) are being developed to overcome these limitations to create living autologous structures that are biocompatible and tailor-made, and that may exhibit the capacity to grow and remodel.[3]

A common approach begins with a biodegradable synthetic preshaped carrier or scaffold,[4] formed like an artery, which is seeded with cells.[5,6] This scaffold functions as a temporary matrix for cell support and anchorage until seeded cells produce their own extracellular matrix proteins. Many differentiated and progenitor cell types have been utilized for cell seeding: autologous endothelial progenitor cells (EPCs) and bone marrow–derived mesenchymal stem cells (MSCs) have been utilized in this report and others,[7] as they provide antithrombotic and extracellular matrix–producing functions, respectively, thereby resembling the native cell types found in a small-diameter artery.[6,8,9] After an *in vitro* stage of tissue-engineered construct conditioning,[10] the vascular construct can be implanted, followed by an *in vivo* stage of scaffold degradation and tissue remodeling intended to recapitulate normal tissue architecture and function.[11] Although the functional feasibility of using TEVGs has been established,[5,12] the mechanisms underlying formation of neovascular tissue and the remodeling of these grafts remain unclear.

Molecular imaging techniques have been used to investigate a number of different biological processes *in vivo*.[13,14] Remodeling of neovascular tissue is mirrored by the degradation and synthesis of extracellular matrix and has shown to be largely mediated by matrix-degrading enzymes (matrix

[1]Center for Molecular Imaging Research, Massachusetts General Hospital, Harvard Medical School, Boston, Massachusetts.
[2]Children's Hospital, Harvard Medical School, Boston, Massachusetts.
*These two authors contributed equally to this work.

metalloproteinases [e.g., MMP-1, MMP-2, MMP-9, and MMP-13] and cysteine proteases [e.g., cathepsins S, K, and B]). Activated vascular cells overexpress MMPs and cathepsins, which, depending on the experimental or clinical scenario, may represent ongoing tissue development, remodeling, or disease progression.[15,16] Using molecular imaging approaches, we recently detected endothelial cell activation, MMP, and cathepsin activity in normal and atherosclerotic mouse aortas and aortic valves.[15,17] Current imaging modalities are able to detect *in vivo* expression and activity of molecules responsible for vascular remodeling and can monitor remodeling of native vascular tissue in individual patients.[18,19]

Considerable research in the field of tissue engineering has relied on using large animal models;[20,21] which are intrinsically limited by the lack of genetically modified strains resulting in an inability to investigate tissue engineering (TE) applications of human-derived cell sources. Several studies have also demonstrated the feasibility of utilizing immunodeficient mice as a reliable tool to study small-caliber TEVGs.[22–24] However, these studies have not addressed important questions regarding the late fate of engrafted cells and *in vivo* TEVG remodeling over time. A recent report used magnetic resonance imaging to monitor TEVGs seeded with iron-oxide nanoparticle–labeled cells.[25] While this study provided important functional and anatomical information, it did not offer biological information at the cellular and molecular levels.

The inability to understand real-time dynamic remodeling processes and cellular changes in tissue engineered structures accounts for the limited knowledge in the field. In the present study, we used a small animal model and different imaging tools to address the specific questions concerning TEVG maturation *in vivo*. We aimed to investigate the dynamic remodeling capability of TEVGs by observing *in vivo* proteolytic enzyme activity otherwise undetectable by conventional imaging modalities. This method additionally offers the advantage of data collection in real time, without animal sacrifice. The secondary goal of this study was to trace *in vivo* the fate of engrafted cells. The results of the present study provide new insights into biology of implanted TEVGs and may aid in the exploration of novel diagnostic imaging strategies.

Materials and Methods

Study design

TEVGs (1 mm diameter) were made from 50% polyglycolic acid (PGA), 50% poly-L-lactic acid (PLLA) nonwoven scaffolds, seeded with green fluorescent protein (GFP)–labeled human bone marrow–derived MSCs and EPCs. They were subsequently implanted into carotid arteries of nude mice ($n = 9$) and evaluated using intravital molecular imaging and histological approaches (Fig. 1). To target key molecular processes involved in tissue remodeling of implanted grafts, we used Prosense680 (VisEn, Woburn, MA) to image cathepsin protease activity. Intravital Microscopy (IV100; Olympus, Tokyo, Japan) was performed postoperative follow-up on mice with implanted grafts, who were anesthetized with 2% isofluorane anesthesia at the time of implantation ($n = 3$) and after 7 ($n = 3$) and 35 ($n = 3$) days postimplantation. After imaging, mice were euthanized and the grafts were explanted for histological evaluation. All experimental procedures were approved by Institutional Animal Care and Use Committee of Children's Hospital.

Tissue engineering of vascular graft

Cells. Human MSCs were isolated from the mononuclear cell fraction of a 25 mL commercially available human bone marrow sample (Lonza, Walkersville, MD).[26] Cells were seeded on 1% gelatin–coated tissue culture plates using endothelial growth medium (EGM-2) (except for hydrocortisone, vascular endothelial growth factor, beta fibroblast growth factor [βFGF], and heparin; Lonza), 20% fetal bovine serum (FBS) (Hyclone, Logan, UT), 1× glutamine–penicillin–streptomycin (GPS; Invitrogen, Carlsbad, CA), and 15% autologous plasma. Unbound cells were removed at 48 h, and the bound cell fraction maintained in culture until 70% confluence using MSC medium: EGM-2 (except for hydrocortisone, vascular endothelial growth factor, βFGF, and heparin), 20% FBS, and 1× GPS. Thereafter, MSCs were subcultured on fibronectin-coated (1 μg/cm^2; Chemicon International, Temecula, CA) plates using MSC medium. MSCs between passages 4 and 9 were used for all the experiments. The characterization of the MSCs was performed as de-

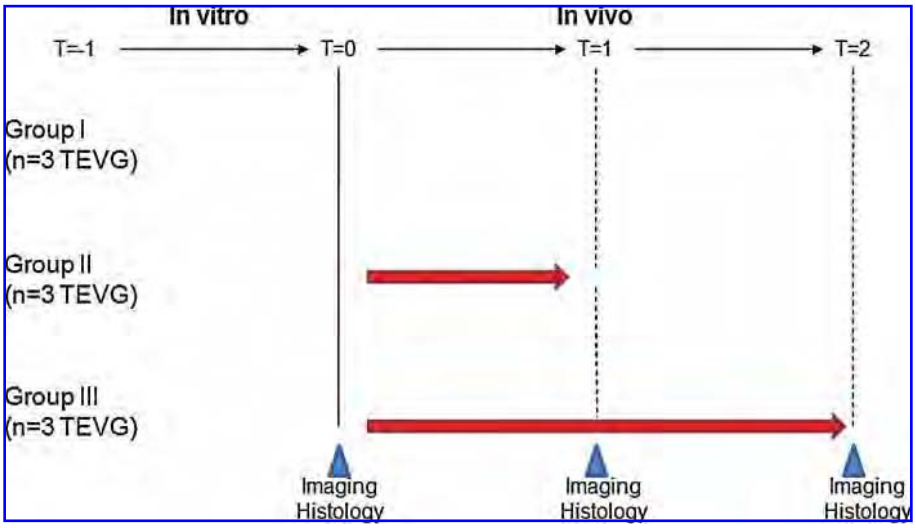

FIG. 1. Study design. *In vitro* phase—T = −1: cell isolation, tissue-engineered vascular construct creation. *In vivo* phase—T = 0: preimplantation; T = 1: 7 days; T = 2: 35 days postimplantation. Color images available online at www.liebertonline.com/ten.

scribed in previous studies.[26,27] The Harvard Committee on Microbiological Safety approved a protocol to work with human bone marrow–derived MSCs.

Retroviral transduction of MSCs. GFP-labeled cells were generated by retroviral infection with a pMX-GFP vector using a modified protocol from Kitamura *et al.*[28] Briefly, retroviral supernatant from HEK 293T cells transfected with Fugene reagent was harvested, and MSCs (1×10^6 cells) were then incubated with 5 mL of virus stock for 6 h in the presence of 8 μg/mL polybrene. GFP-expressing cells were sorted by fluorescence-activated cell sorting (FACS), expanded under routine conditions, and used for *in vivo* experiments.

Isolation and culture of EPCs. Human umbilical cord blood was obtained from the Brigham and Women's Hospital in accordance with an Institutional Review Board–approved protocol. EPCs were isolated from the mononuclear cell fraction of cord blood samples, and purified using CD31-coated magnetic beads as previously described.[29] EPCs were subcultured on fibronectin-coated plates using EPC medium: EGM-2 (except for hydrocortisone) supplemented with 20% FBS (Hyclone), 1× GPS. EPCs between passages 5 and 7 were used for all the experiments.

Scaffold. Imaging studies of complex tissues require use of polymers with minimal autofluorescent potential in 488, 633, and 748 nm wavelength channels. We, therefore, first imaged several scaffold candidates (PGA-PLLA; Concordia, Coventry, RI; poly-4-hydroxybutyrate [P4HB] and P4HB-film; Tepha, Lexington, MA) without cell seeding. The gray values in all channels were subsequently quantified and subjected to statistical analysis using analysis of variance to compare differences between groups ($p < 0.05$). The difference between P4HB and P4HB-film is that the nonwoven mesh is extruded as fibers and then laid into a mesh, and the film is melted into a film. The mesh is very porous and the film is essentially nonporous. In addition, the P4HB-film produces high fluorescence signals in all channels, and therefore could not be used for imaging. In contrast, the PGA-PLLA scaffold showed minimum fluorescence as validated by quantification analysis (Fig. 3) and as such was selected as the candidate for this imaging study. In addition to low autofluorescence, the PGA-PLLA polymers have sufficient tensile strength for implantation into the circulation[23] and acceptable biomechanical properties, porosity and biocompatibility, to function as an arterial graft as previously described.[9,10,20] We therefore constructed the small-diameter biodegradable tubular scaffolds using 50% PGA, 50% PLLA nonwoven polymers. Nine tubular scaffolds of ~1 mm in inner diameter, ~1.3 mm in outer diameter (comparable to carotid artery diameter of mouse model), and 5 mm in length were constructed.

Construct development. PGA-PLLA scaffolds were cannulated with a plastic cannula (Angiocath, 20G; Wilburn Medical, Kernesville, NC) and sterilized via ethylene oxide gas. Scaffolds were prewet with 70% ethanol, washed ×3 with sterile phosphate-buffered saline (PBS), and then incubated in a solution of FBS and antibiotics (10×) for 2–3 h while cells were prepared. MSC/EPC coculture was initially seeded in a ratio of 3:1 onto the scaffold by directly pipetting cells onto the scaffold, and then changing medium daily. One end of the scaffold was occluded with a sterile surgical clip and pipetting the cell suspension into the lumen through the opposite end. After the initial seeding period, each graft was incubated for 9 days in 80 mL of Dulbecco's modified Eagle's medium (DMEM) with 20% FBS, 10 mM 4-(2-hydroxyethyl)-1-piperazineethanesulfonic acid (HEPES), 2 ng/mL βFGF, 80 μg/mL of ascorbic acid-2-phosphate, and 1× antibiotic/antimycotic, which was changed every 3–4 days. The angiocatheter was replaced in the lumen on culture day 9 to prevent occlusion due to cellular ingrowth. On culture day 10, the angiocatheter was removed and ~6×10^6 EPCs were pipetted into the lumen of the graft by applying a surgical clip to one end of the graft, pipetting cells into the lumen, and then applying a clip to the other end of the graft. To allow for endothelial cell adhesion, the graft sat for 10 min before submersion in medium, 24 h before surgical implantation.[11,23]

Surgical implantation of TEVGs in nude mice

TEVGs were implanted in the right common carotid artery of 12-week-old nude mice under 2% isofluorane anesthesia. A right longitudinal cervicotomy was made; using a dissecting microscope, the right common carotid artery was then separated from the left vagus nerve using fine-tipped dissecting forceps. Two vascular clamps were used to stop the carotid artery flow; a proximal clamp was placed 10 mm from the bifurction of the common carotid artery, and a distal clamp was applied at the bifurcation. After flow was occluded, the right common carotid artery between the two clamps was excised and replaced with the TEVGs, via end-to-end anastomoses created using 10-0 monofilament nylon sutures. The wound was closed with running 7-0 prolene sutures. There were no known complications or mortality during the surgical graft implantation.

Near-infrared imaging agents

Remodeling potential. The activity of matrix-degrading enzymes in the TEVGs was assessed by a near-infrared (NIR) protease-activatable imaging probe (Prosense; ex 680; VisEn) injected intravenously 24 h before imaging (2 nmol/150 μL in PBS). The agent has been validated in a mouse model for tissue remodeling that revealed activity of cysteine proteases (predominantly cathepsin B).[15] These quenched substrate probes produce negligible fluorescence at baseline because of closely spaced fluorochromes. However, on protease-mediated cleavage and fluorochrome release, the NIR signal increases by ~200-fold.

Function. Blood pooling NIR fluorescence imaging probes have been widely used to image the vasculature of different organs in various disease processes,[30] serving as a tool for studying coronary circulation and cardiac function.[31] In general, these agents circulate in the blood up to 2 h, allowing the imaging of vessels. We used blood pooling NIR agent to assesses the blood flow through surgical anastomoses (Angiosense; ex 750; VisEn) injected at the time of imaging (10 nmol/150 μL in PBS).

Microscopic laser scanning fluorescence imaging

Microscopic fluorescence imaging was performed with a laser scanning fluorescence microscope specifically developed

for imaging small experimental animals (IV100; Olympus). We first imaged unimplanted seeded scaffolds to detect initial cellular GFP signal. Then, mice were imaged at time 0 ($n = 3$), 7 ($n = 3$), and 35 ($n = 3$) days after TEVG implantation. Mice were injected via tail vein with Prosense680 (VisEn) 24 h before imaging and with Angiosense750 (VisEn) during imaging. TEVGs were excited at 488, 633, and 748 nm and images collected in three separate channels using dichronic mirror SDM 570 ad SDM 750 and emission filters BA 505–550 for GFP, BA 650–700 for Prosense680, and BA 770 LP for Angiosense750. Images of 512×512 pixels with a pixel size of 2.75×2.75 μm/pixel were collected with the FluoView300 software program (Olympus) and stored as multilayer, 16-bit tagged image file format (TIFF) files as previously described by our group.[15,32] To avoid cross talk between channels, image collection was done serially. Images were processed and analyzed with ImageJ computer software (version 1.41; Bethesda, MD). After *in vivo* imaging, TEVGs were excised for direct NIR fluorescence microscopy and histopathological analyses. All imaging procedures were approved by the subcommittee on Research Animal Care at Massachusetts General Hospital.

Correlative histological assessment

Morphological characterization. Tissue samples were frozen in optimal cutting temperature (OCT) compound (Sakura Finetech, Torrance, CA), and 5 μm serial sections were cut through the TEVGs. All grafts were stained with hematoxylin and eosin for general morphology, Masson trichrome stain for collagen organization, and von Geison for elastin formation.

NIR fluorescence microscopy. We performed direct NIR fluorescence microscopy to validate GFP signal and proteolytic activity, representing the remodeling process. Fresh cryosections through TEVGs were imaged with an upright epifluoresence microscope (Eclipse 80i; Nikon Instruments, Melville, NY) with a cooled CCD camera (Cascade; Photometrics, Tucson, AZ). Fluorescence images were then obtained for GFP signal using filter (480 ± 20 nm excitation and 535 ± 25 nm emission) and for Prosense with filter (650 ± 22.5 nm excitation and 710 ± 25 nm emission). The exposure time ranged from 200 to 500 ms.

Immunohistochemistry. To validate the cellular phenotype and proteolytic enzyme expression, immunohistochemistry for myofibroblasts (α-smooth muscle actin, 1A4; Dako, Carpinteria, CA), endothelial cells (anti-mouse CD31 and anti-human CD31; Dako), mouse macrophages (mac-3; BD Biosciences, San Jose, CA), cathepsin B (goat polyclonal antibodies; Santa Cruz Biotechnology, Santa Cruz, CA), and gelatinases (polyclonal rabbit anti-mouse MMP-2 and MMP-9; Chemicon International) was used. The avidin–biotin peroxidase method was performed for immunohistochemistry. The reaction was observed with a 3-amino-9-athyl-carbazol substrate (AEC Sigma Chemical, St. Louis, MO), which yielded red reaction products. Images were captured with a digital camera (Nikon DXM 1200-F; Nikon Instruments).

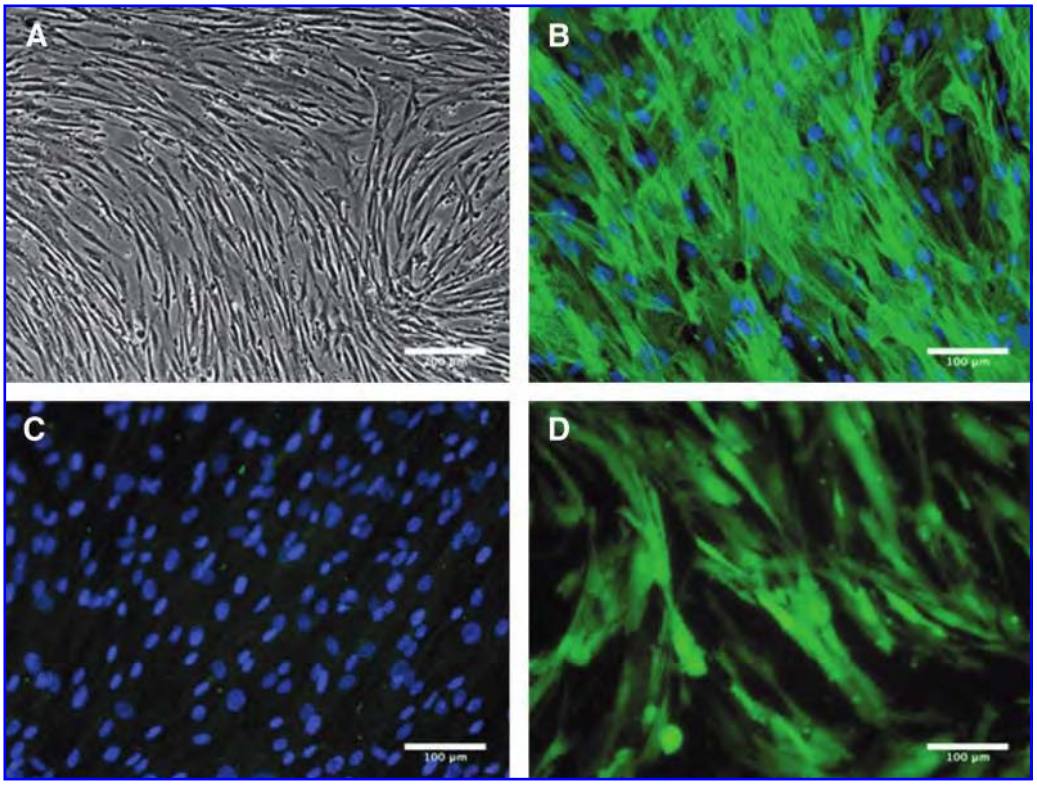

FIG. 2. MSC characterization preseeding. (**A**) Phase contrast photomicrograph shows morphology of MSCs; (**B**) MSC immunostaining with α-SMA; (**C**) MSC immunostaining with CD31, nuclei stain with 4,6′-diamidino-2-phenylindole (DAPI); (**D**) GFP-labeled MSCs. MSCs, mesenchymal stem cells; α-SMA, alpha-smooth muscle actin; GFP, green fluorescent protein. Color images available online at www.liebertonline.com/ten.

Results

Characterization of MSCs and retroviral transfection with GFP

MSCs were isolated from the mononuclear cell fractions of human bone marrow samples as previously described.[29] MSCs adhered rapidly to the culture plates, proliferated with ease until confluent, and presented spindle morphology characteristic of mesenchymal cells in culture (Fig. 2A).[30] The phenotype of the MSCs was confirmed by indirect immunofluorescent staining: MSCs were shown to express the mesenchymal marker α-smooth muscle actin (Fig. 2B) but not the endothelial marker CD31 (Fig. 2C). The ability of MSCs to differentiate into multiple mesenchymal lineages was also detected *in vitro* using well-established protocols.[30] Differentiation of MSCs into adipocytes, osteocytes, and chondrocytes was confirmed by Oil red O staining (adipogenesis), expression of alkaline phosphatase (osteogenesis), and glycosaminoglycan deposition in pellet cultures (chondrogenesis), respectively (data not shown). Finally, MSCs were retrovirally transfected to ubiquitously express GFP (Fig. 2D) before their use *in vivo*.

PGA-PLLA is a suitable scaffold

To determine which scaffold would be more appropriate for use in intravital imaging experiments, different scaffold polymer materials (PGA-PLLA, P4HB, and P4HB-film) were imaged and gray values of the fluorescence intensity were analyzed to evaluate their fluorescence properties (Fig. 3). PGA-PLLA showed the least amount of fluorescence in 488 and 633 nm wavelength, the channels used for imaging of GFP-labeled MSCs and remodeling proteins, respectively (Fig. 3A, D). P4HB-based materials showed considerable fluorescence in all three channels (Fig. 3B–D). As such, using PGA-PLLA scaffold material in the construct would provide for the least amount of interfering signal when imaging TEVGs *in vivo*.

Tissue-engineered constructs show tissue formation before implantation

Histological analysis of the cryosections obtained from cell-seeded tissue-engineered constructs before implantation demonstrated organized tissue formation and an endothelial monolayer in the lumen (Fig. 4A, B). The polymers had

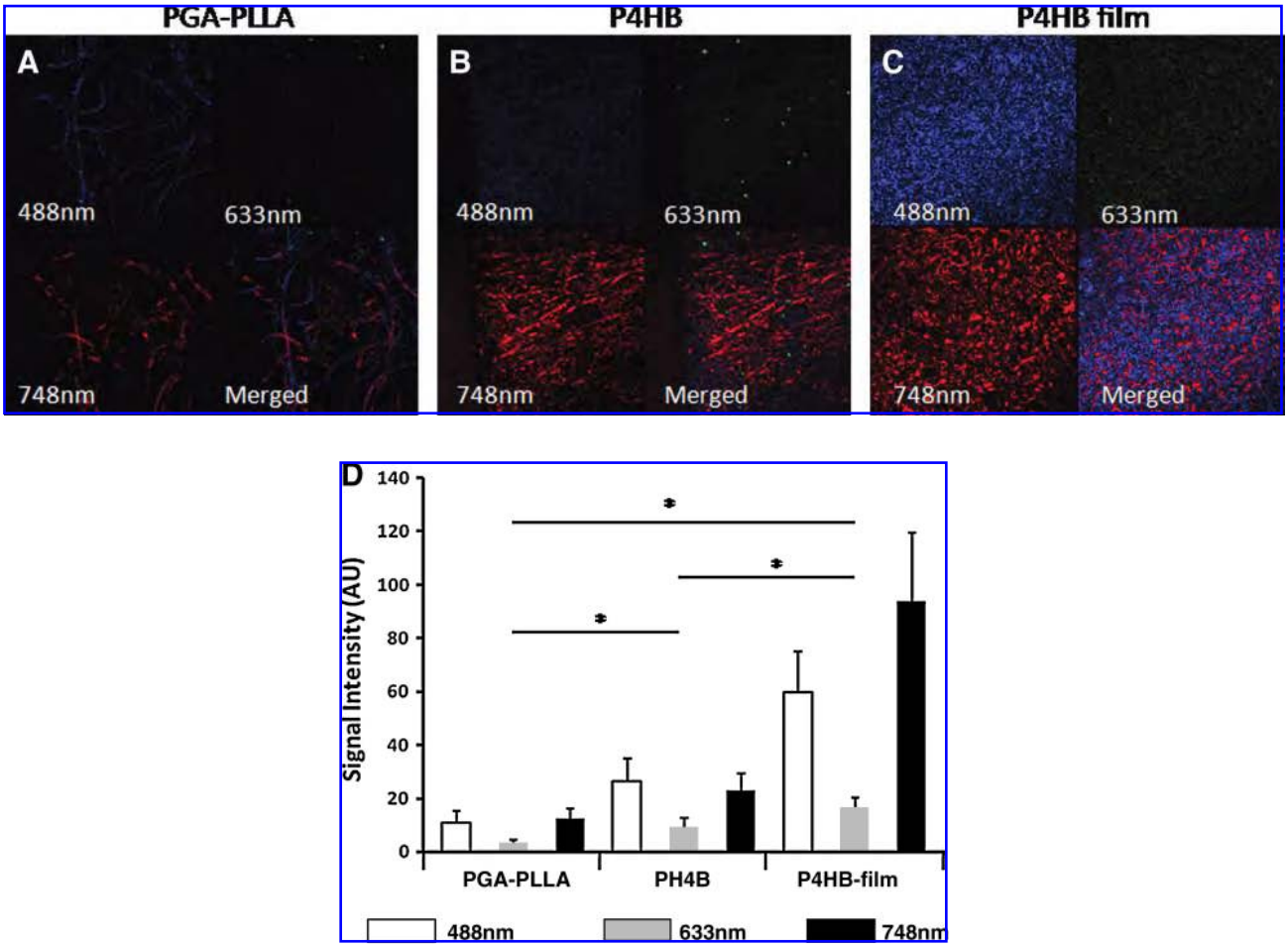

FIG. 3. Imaging of scaffold materials. (**A**) PGA-PLLA; (**B**) P4HB; (**C**) P4HB-film. (**D**) Quantitative analysis of signal intensities demonstrates that PGA-PLLA have significantly less fluorescence in all channels (*$p < 0.05$). Fluorescence channels: blue, 488 nm; green, 633 nm; red, 748 nm. PGA, polyglycolic acid; PLLA, poly-L-lactic acid; P4HB, poly-4-hydroxybutyrate. Color images available online at www.liebertonline.com/ten.

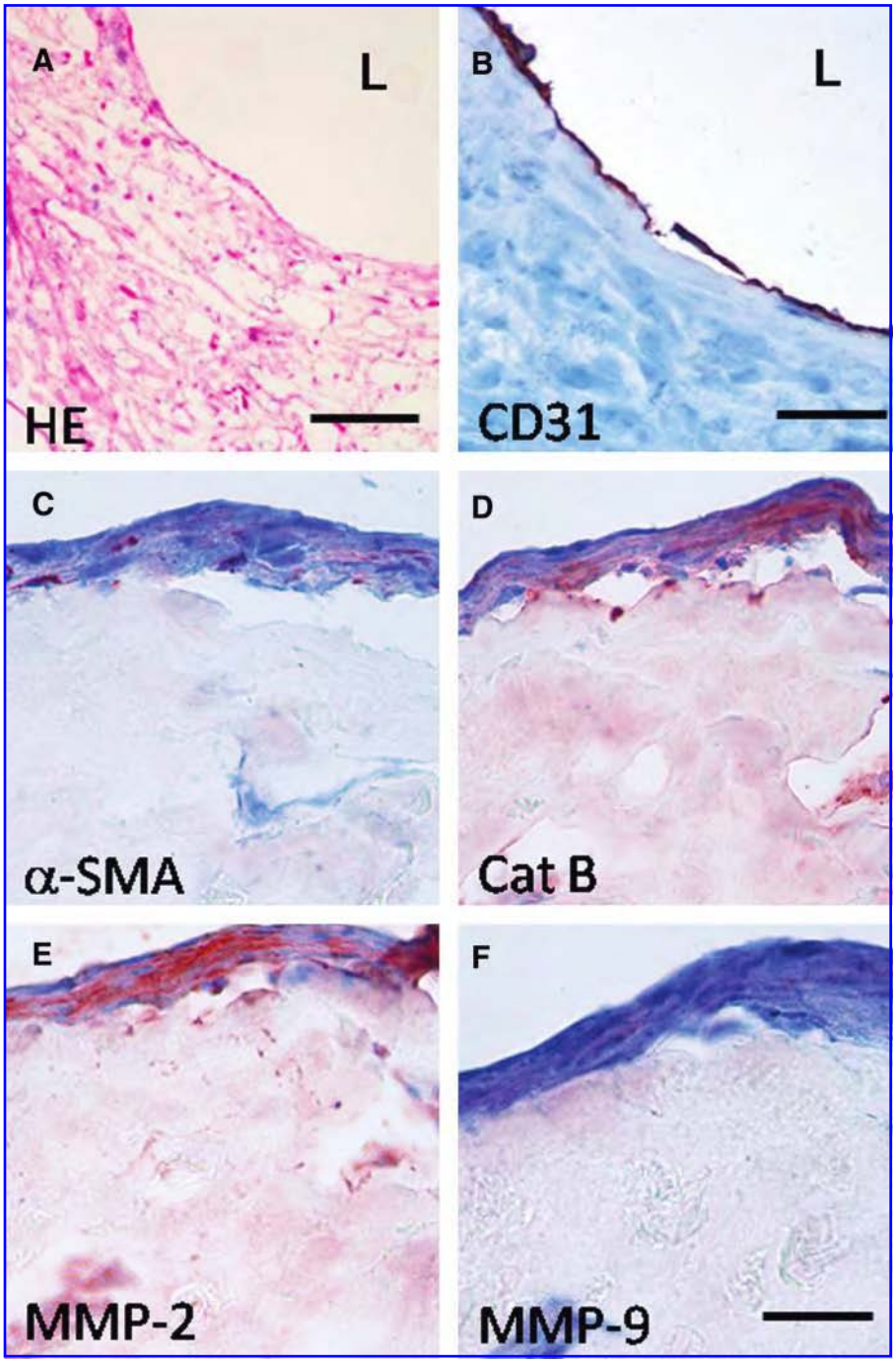

FIG. 4. Histological evaluation of preimplanted constructs. (**A**) HE, bar = 200 μm; (**B**) CD31, bar = 100 μm; (**C**) α-SMA; (**D**) Cathepsin B; (**E**) MMP-2; (**F**) MMP-9. Bar = 50 μm; L = lumen. HE, hematoxylin and eosin; MMP, matrix metalloproteinase. Color images available online at www.liebertonline.com/ten.

degraded minimally before implantation. Further immunohistochemical analysis indicated α-smooth muscle actin–positive myofibroblast-like cell phenotype (Fig. 4C) and expression of remodeling enzymes such as cathepsin B, MMP-2, and MMP-9 (Fig. 4D–F).

Remodelling of tissue-engineered constructs validated by imaging

Intravital multichannel laser scanning fluorescence microscopy was used to observe real-time *in vivo* remodeling activity of TEVGs before implantation, immediately after implantation, and at 7 and 35 days after implantation (Fig. 5; green: GFP, ex 488; red: Prosense680, ex 633; blue: Angiosense750, ex 748). Imaging of the preimplanted TE construct demonstrated GFP-positive cells on the surface and throughout the scaffold, but no proteolytic cathepsin activity (Fig. 5C). Immediately after implantation, grafts showed strong GFP signal (green) on the graft surface, adequate patency of the graft anastomosis detected by Angiosense (blue), and demonstrated a larger diameter of the TE graft than the native artery, consistent with the macroscopic appearance of the graft (Fig. 5D). At day 7, the grafts showed patchy GFP signal (green) and strong protease activity (red) indicating an active remodeling process (Fig. 5E). At 35 days, implants demonstrated predominantly proteolytic activity and less

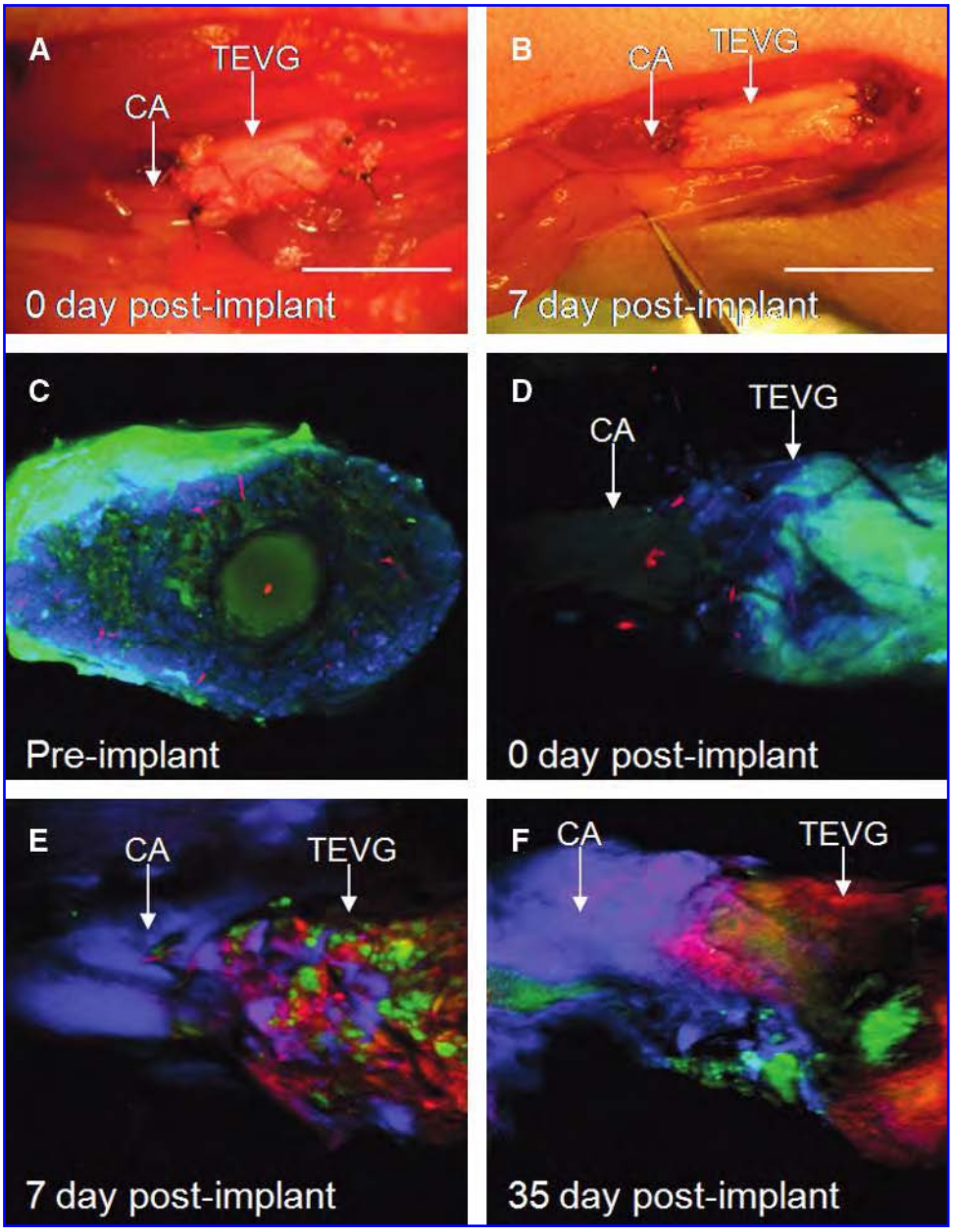

FIG. 5. Imaging of TEVGs. (**A**) Macroscopic pictures of native carotid artery and TEVGs at implantation. (**B**) Surgical field of implanted TEVGs at 7 day after implantation. (**C**) Intravital molecular imaging of TEVGs at the time before implantation (cross section). (**D–F**) Intravital molecular imaging of TEVGs (site of anastomosis) immediately after implantation (**D),** and 7 days (**E**) and 35 days (**F**) postimplantation (green, GFP; red, Prosense680; blue, Angiosense750). CA, mouse carotid artery; TEVGs, tissue-engineered vascular grafts. Color images available online at www.liebertonline.com/ten.

GFP-positive cells, suggesting that the original MSCs were likely replaced by other cells (Fig. 5F). Intravital imaging clearly detected the signal from a blood pooling imaging agent at the anastomoses of 7- and 35-day implants (Fig. 5E, F). Using this imaging approach, we could show that all implanted grafts were patent. However, the limitation of this method is that intravital microscopy cannot penetrate through the thickened wall of the polymer-based tissue-engineered constructs, and for that reason, we cannot assure that all grafts were clear of obstruction.

TEVG remodeling validated by histology

NIR imaging of the tissue-engineered graft 7 days after implantation showed increased remodeling detected by proteolytic enzyme activity (Prosense680; Fig. 6A). Histological analysis revealed layered vascularized tissue and the presence of diffusely distributed macrophages detected by murine mac-3 antibody (Fig. 6B–E). Lumen endothelization was not consistently present (Fig. 6D). Importantly, cathepsin B expression was prominent in the majority of cells, corroborating NIR imaging findings (Fig. 6F). Expression of MMP-2, particularly, MMP-9, was found in fewer cells (Fig. 6G, H).

Fluorescence NIR microscopy (Prosense680) registered active remodeling of TEVGs at 35 days (Fig. 7A). TEVGs showed distinct layers of organized cells (Fig. 7B), collagen on the surface (Fig. 7C), and sparse endothelization (Fig. 7D). Elastin was not detected (data not shown). In addition, the macrophages were more sparse and appeared to form clusters (Fig. 7E). Remodeling enzymes, particularly, cathepsin B and MMP-9, were abundantly present at this stage (Fig. 7F–H). Of note, the difference between MMP-2 and MMP-9 expression was more prominent than after 7 days, indicating that MMP-9 is actively involved in late remodeling. The anastomosis lumen showed no indication of thrombus formation (Fig. 7I).

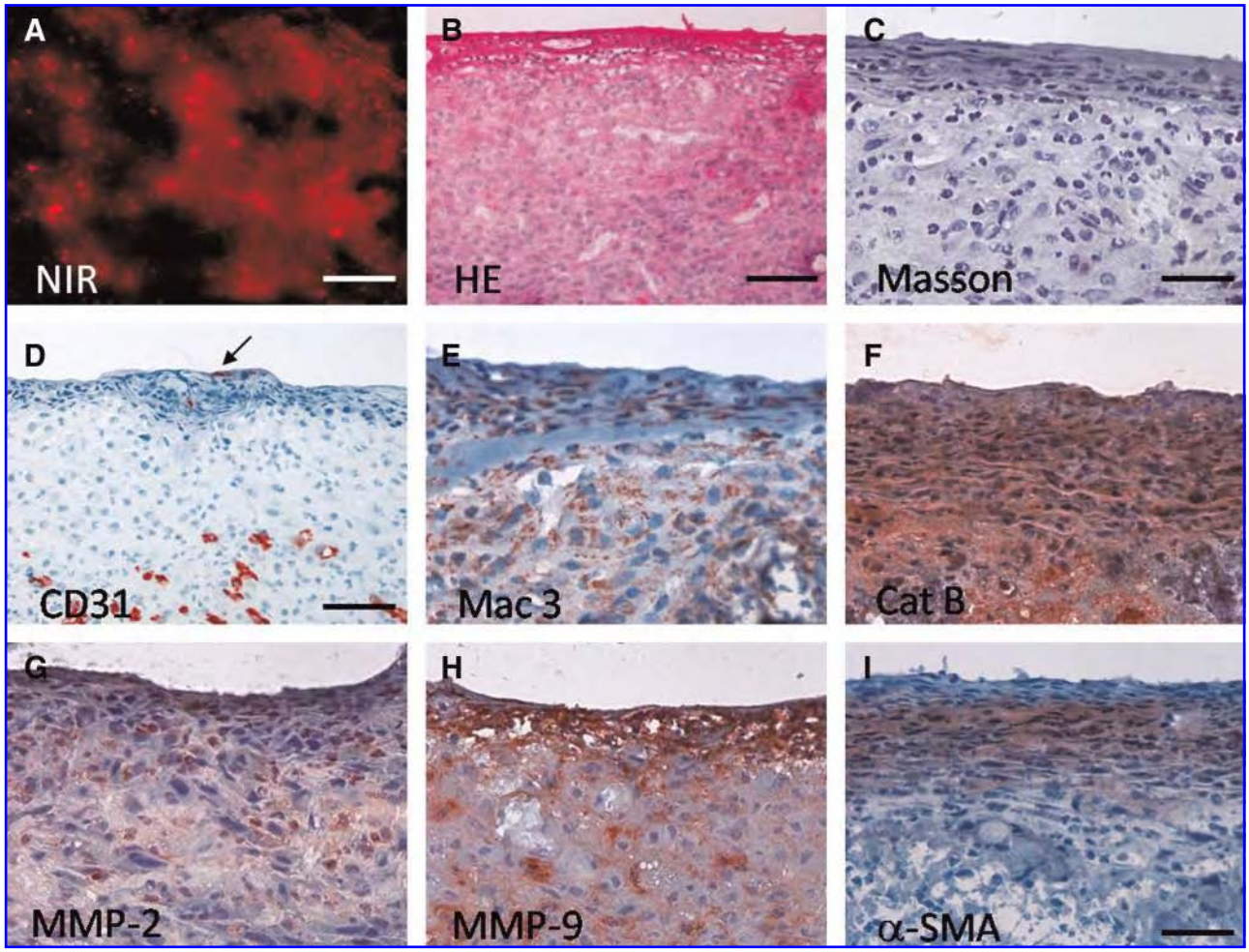

FIG. 6. Remodeling of TEVGs 7 days after implantation. (**A**) NIR fluorescent imaging exhibited proteolytic activity on the sections through TEVGs at 7 day explant; (red, Prosense680); bar = 50 μm. HE and immunohistochemistry correlated with NIR signal. (**B**) HE, bar = 100 μm; (**C**) Masson trichrome, bar = 50 μm; (**D**) CD31 in endothelium (arrow) and microvessels, bar = 100 μm; (**E**) Mac3; (**F**) Cathepsin B; (**G**) MMP-2; (**H**) MMP-9, (**I**) α-SMA. Bar (**E–I**) = 50 μm. NIR, near-infrared. Color images available online at www.liebertonline.com/ten.

GFP-labeling signal is preserved over time

GFP-labeling signal intensity, although decreased, remained present over time (Fig. 8). The number of cells in the TEVGs was qualitatively fewer at 35 days than 7 days, supporting our *in vivo* imaging findings.

Discussion

This study demonstrated that intravital molecular imaging can be utilized to observe the dynamic remodeling processeses of a small-caliber TEVG implanted into mouse systemic circulation. Key findings documented here show (1) that *in vivo* remodeling and maturation of TEVGs could be monitored by NIR protease-activatable imaging agents; (2) GFP labeling of the implanted cells provides a means to track cells over time; and (3) TEVG patency could be monitored simultaneously by introducing fluorescence molecular imaging agents labeling blood pool. (4) In addition, our imaging findings were validated by standard histological methods, and demonstrated that the remodeling process involves and is perhaps initiated by macrophage invasion, and that by day 35, the majority of the initially seeded human MSCs were replaced by host murine cells as detected by immunohistochemistry to mouse-specific antibodies. Over time, the remodeling enzyme activity decreased and grafts displayed layered collagenous tissue.

The tissue engineering paradigm used in our study, in which mononuclear cells derived from bone marrow and seeded on biodegradable polymer scaffolds are used to create a vascular graft, has been previously demonstrated.[6,33–35] Moreover, successful postoperative results have been reported in humans.[5,36] However, studies of the biological and cellular behavior of human cells are warranted. Therefore, using a nude mouse model for this study had a number of benefits. First, the minimized immune response of nude mice allowed us to study human cells as a source for TEVGs.[23,24] In addition, using human cells in preclinical TEVG development has the advantage of identifying biological characteristics of human cells, which could potentially influence their clinical potential.[11] Moreover, a human–mouse chimeric system allows for detailed cell-tracking experiments based on species-specific markers, providing further insights into the cellular

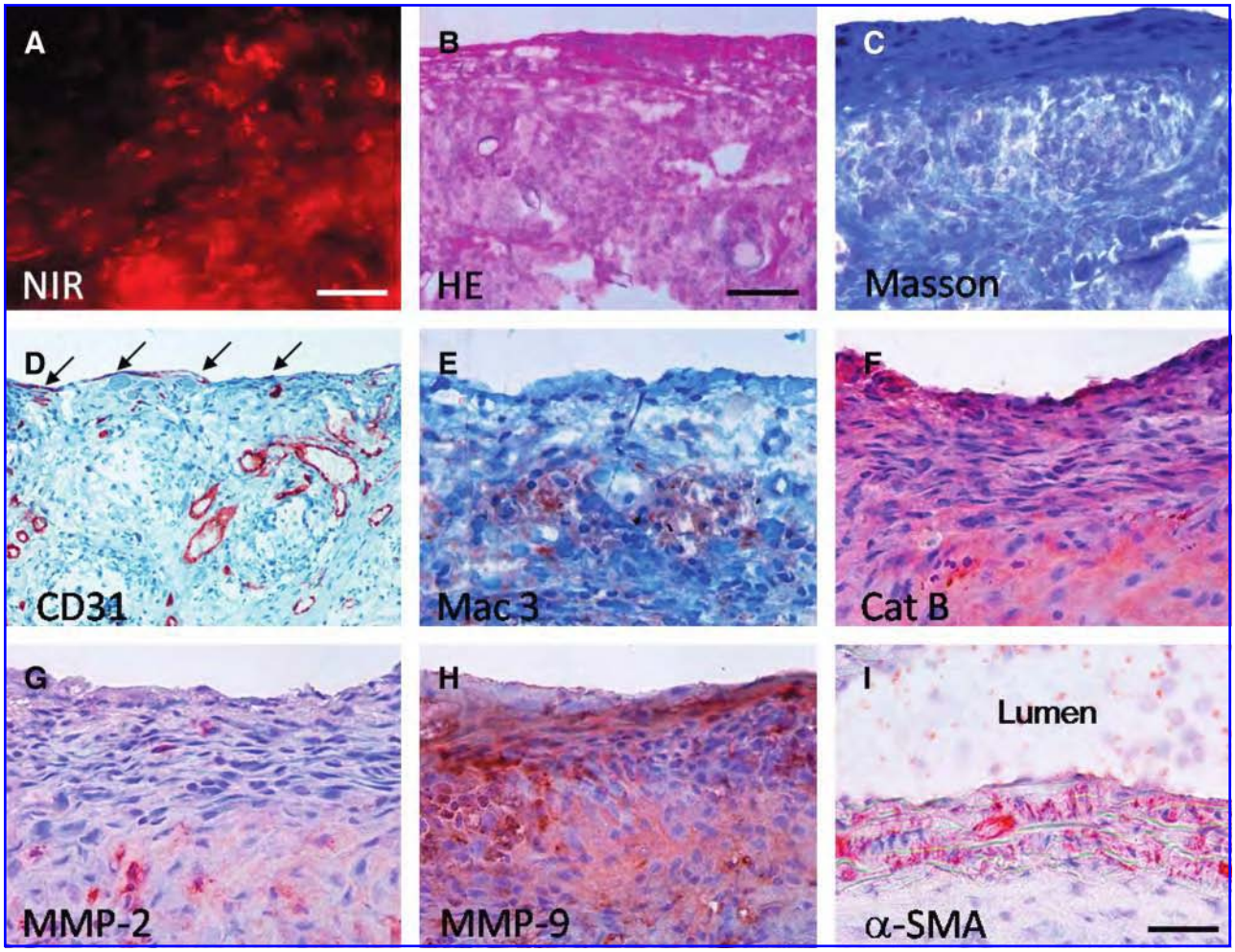

FIG. 7. Remodeling of TEVGs 35 days after implantation. (**A**) NIR fluorescent imaging exhibited proteolytic activity on the sectiones through TEVGs at 35 day explant (red, Prosense680); bar = 50 μm. HE and immunohistochemistry correlated with NIR signal. (**B**) HE, bar = 100 μm; (**C**) Masson trichrome, bar = 50 μm; (**D**) CD31 in endothelium (arrow) and microvessels, bar = 100 μm; (**E**) Mac3; (**F**) Cathepsin B; (**G**) MMP-2; (**H**) MMP-9; (**I**) α-SMA through anastomosis area. Bar (**E–I**) = 50 μm. Color images available online at www.liebertonline.com/ten.

mechanisms involved in vascular neotissue development. There are significant differences between human and murine vascular systems such as size, morphology, and accelerated neointimal hyperplasia (in mice). However, fundamental similarities between both species could allow the translation of findings from a murine model toward clinical application.[22]

The mechanism of vascular neotissue formation in TEVG is largely unknown. Hemodynamic forces in the arterial circulation could play an important role in the remodeling process of the graft by contributing to the recruitment and proliferation of MMP-expressing cells.[37] As in other studies, we observed a significant macrophage infiltration in the TEVG wall,

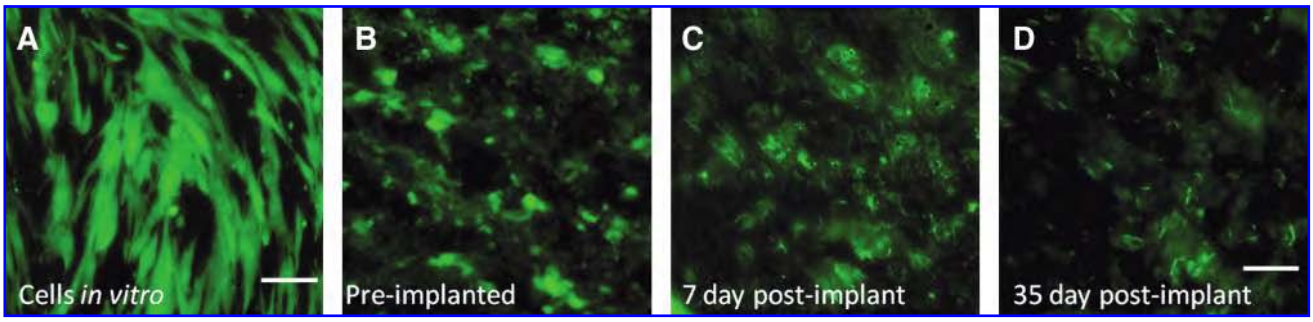

FIG. 8. Overtime changes of GFP signal in MSCs. (**A**) *In vitro* before seeding; bar = 100 μm; (**B**) preimplanted, (**C**) 7 days postimplantation, (**D**) 35 days postimplantation. Bar (**B–D**) = 50 μm. Color images available online at www.liebertonline.com/ten.

implicating a role for inflammation in vascular neotissue formation. Macrophages degrade the extracellular matrix by the secretion of proteases such as cathepsins and MMPs and facilitate their migration through the inflamed tissue. Although MMPs are key mediators of vascular remodeling, there is incomplete data on the biological roles of MMP-2 and MMP-9 activity.[38] MMP-9 overexpression in vascular smooth muscle cells leads to expansive remodeling and thinning of the intima in rat carotid arteries,[39] and in MMP-2 and MMP-9 knockout mice, remodeling and neointima formation are induced by carotid ligation.[40,41]

Nevertheless, MMPs play a major role in the healing process.[41] Moreover, even though macrophage activity can be destructive, this activity seems necessary to promote healing.[41] However, it is difficult to distinguish inflammation as part of a remodeling or a healing process from inflammation as part of an elaborate immune response or disease. In our study, the mouse model lacks a functional T-cell–mediated immune system, which circumvents host-versus-graft rejection; however, it may influence results with regard to remodeling. Prior reports using scaffolds from similar polymers have demonstrated no evidence of an adaptive immune response to the biomaterials used in this study.[23,42] Nude mice exhibit an intact innate immune system, which means that nude mice are capable of mounting a similar inflammatory response to scaffold material like immunocompetent mice.[23] As a result, we conclude that the inflammation demonstrated in this pilot study is a part of remodeling activity inherent to neotissue formation. However, additional studies investigating long-term remodeling and growth of TEVG in a larger number of mice are needed.

In previous studies from our laboratories, we demonstrated promising results in tissue engineering and molecular imaging.[15,20,21,32] Here, we offer a sensitive and specific detection of fluorescent signals that allows for multispectral imaging of biological processes *in vivo* in tissue engineered structures. Specifically, we demonstrated that this imaging approach may serve as an excellent tool to monitor remodeling activity and cell fate in functional TEVGs. Using different NIR fluorescent agents, information about graft maturation, function, and cell fate can be gained from one imaging session. Hence, the model described herein provides benefits for studying neotissue formation of implanted small-diameter TEVGs.

In conclusion, this study has demonstrated the feasibility of evaluating remodeling of TEVGs by means of molecular imaging. A better understanding of the process of neotissue formation is important to the continued development and rationale design of TEVGs. This multidisciplinary experimental approach has the advantage of evaluating remodeling and growth of TEVG *in vivo* and provides a step toward the development of a reliable noninvasive assessment tools with potential clinical utility.[43]

Acknowledgments

This study was supported in part by Wijck-Casper-Stam Foundation (J.H.), U.S. Army Medical Research and Materiel Command (W81XWH-05-1-0115) (J.B.), and AHA 0835460N (E.A.). The authors would like to thank Yoshiko Iwamoto for excellent histological technique, Dr. Soo-Young Kang for assistance with the retroviral transfection of the cells, and David Martin (Tepha) for providing P4HB-based scaffold samples.

Disclosure Statement

No competing financial interests exist.

References

1. DeFrances, C.J., Lucas, C.A., Buie, V.C., and Golosinskiy, A. 2006 National Hospital Discharge Survey. Natl Health Stat Report 2008(5):1–20.
2. Dearani, J.A., Danielson, G.K., Puga, F.J., Schaff, H.V., Warnes, C.W., Driscoll, D.J., Schleck, C.D., and Ilstrup, D.M. Late follow-up of 1095 patients undergoing operation for complex congenital heart disease utilizing pulmonary ventricle to pulmonary artery conduits. Ann Thorac Surg **75,** 399–410; discussion 410–391, 2003.
3. L'Heureux, N., McAllister, T.N., and de la Fuente, L.M. Tissue-engineered blood vessel for adult arterial revascularization. N Engl J Med **357,** 1451, 2007.
4. Rabkin, E., and Schoen, F.J. Cardiovascular tissue engineering. Cardiovasc Pathol **11,** 305, 2002.
5. Shin'oka, T., Matsumura, G., Hibino, N., Naito, Y., Watanabe, M., Konuma, T., Sakamoto, T., Nagatsu, M., and Kurosawa, H. Midterm clinical result of tissue-engineered vascular autografts seeded with autologous bone marrow cells. J Thorac Cardiovasc Surg **129,** 1330, 2005.
6. Roh, J.D., Brennan, M.P., Lopez-Soler, R.I., Fong, P.M., Goyal, A., Dardik, A., and Breuer, C.K. Construction of an autologous tissue-engineered venous conduit from bone marrow-derived vascular cells: optimization of cell harvest and seeding techniques. J Pediatr Surg **42,** 198, 2007.
7. Kaushal, S., Amiel, G.E., Guleserian, K.J., Shapira, O.M., Perry, T., Sutherland, F.W., Rabkin, E., Moran, A.M., Schoen, F.J., Atala, A., Soker, S., Bischoff, J., and Mayer, J.E., Jr. Functional small-diameter neovessels created using endothelial progenitor cells expanded *ex vivo*. Nat Med **7,** 1035, 2001.
8. Shinoka, T. Tissue engineered heart valves: autologous cell seeding on biodegradable polymer scaffold. Artif Organs **26,** 402, 2002.
9. Schmidt, D., Asmis, L.M., Odermatt, B., Kelm, J., Breymann, C., Gossi, M., Genoni, M., Zund, G., and Hoerstrup, S.P. Engineered living blood vessels: functional endothelia generated from human umbilical cord-derived progenitors. Ann Thorac Surg **82,** 1465–1471; discussion 1471, 2006.
10. Mirensky, T.L., and Breuer, C.K. The development of tissue-engineered grafts for reconstructive cardiothoracic surgical applications. Pediatr Res **63,** 559, 2008.
11. Nelson, G.N., Mirensky, T., Brennan, M.P., Roh, J.D., Yi, T., Wang, Y., and Breuer, C.K. Functional small-diameter human tissue-engineered arterial grafts in an immunodeficient mouse model: preliminary findings. Arch Surg **143,** 488, 2008.
12. Shin'oka, T., Imai, Y., and Ikada, Y. Transplantation of a tissue-engineered pulmonary artery. N Engl J Med **344,** 532, 2001.
13. Jaffer, F.A., Libby, P., and Weissleder, R. Molecular imaging of cardiovascular disease. Circulation **116,** 1052, 2007.
14. Sosnovik, D.E., Nahrendorf, M., and Weissleder, R. Magnetic nanoparticles for MR imaging: agents, techniques and cardiovascular applications. Basic Res Cardiol **103,** 122, 2008.
15. Aikawa, E., Nahrendorf, M., Sosnovik, D., Lok, V.M., Jaffer, F.A., Aikawa, M., and Weissleder, R. Multimodality molecular imaging identifies proteolytic and osteogenic activities in early aortic valve disease. Circulation **115,** 377, 2007.
16. Deguchi, J.O., Aikawa, E., Libby, P., Vachon, J.R., Inada, M., Krane, S.M., Whittaker, P., and Aikawa, M. Matrix metalloproteinase-13/collagenase-3 deletion promotes col-

lagen accumulation and organization in mouse atherosclerotic plaques. Circulation **112,** 2708, 2005.
17. Deguchi, J.O., Aikawa, M., Tung, C.H., Aikawa, E., Kim, D.E., Ntziachristos, V., Weissleder, R., and Libby, P. Inflammation in atherosclerosis: visualizing matrix metalloproteinase action in macrophages *in vivo*. Circulation **114,** 55, 2006.
18. Jaffer, F.A., Libby, P., and Weissleder, R. Molecular and cellular imaging of atherosclerosis: emerging applications. J Am Coll Cardiol **47,** 1328, 2006.
19. Nahrendorf, M., Sosnovik, D.E., and Weissleder, R. MR-optical imaging of cardiovascular molecular targets. Basic Res Cardiol **103,** 87, 2008.
20. Sutherland, F.W., Perry, T.E., Yu, Y., Sherwood, M.C., Rabkin, E., Masuda, Y., Garcia, G.A., McLellan, D.L., Engelmayr, G.C., Jr., Sacks, M.S., Schoen, F.J., and Mayer, J.E., Jr. From stem cells to viable autologous semilunar heart valve. Circulation **111,** 2783, 2005.
21. Sodian, R., Hoerstrup, S.P., Sperling, J.S., Daebritz, S., Martin, D.P., Moran, A.M., Kim, B.S., Schoen, F.J., Vacanti, J.P., and Mayer, J.E., Jr. Early *in vivo* experience with tissue-engineered trileaflet heart valves. Circulation **102(19 Suppl 3),** III22, 2000.
22. Goyal, A., Wang, Y., Su, H., Dobrucki, L.W., Brennan, M., Fong, P., Dardik, A., Tellides, G., Sinusas, A., Pober, J.S., Saltzman, W.M., and Breuer, C.K. Development of a model system for preliminary evaluation of tissue-engineered vascular conduits. J Pediatr Surg **41,** 787, 2006.
23. Roh, J.D., Nelson, G.N., Brennan, M.P., Mirensky, T.L., Yi, T., Hazlett, T.F., Tellides, G., Sinusas, A.J., Pober, J.S., Saltzman, W.M., Kyriakides, T.R., and Breuer, C.K. Small-diameter biodegradable scaffolds for functional vascular tissue engineering in the mouse model. Biomaterials **29,** 1454, 2008.
24. Lopez-Soler, R.I., Brennan, M.P., Goyal, A., Wang, Y., Fong, P., Tellides, G., Sinusas, A., Dardik, A., and Breuer, C. Development of a mouse model for evaluation of small diameter vascular grafts. J Surg Res **139,** 1, 2007.
25. Nelson, G.N., Roh, J.D., Mirensky, T.L., Wang, Y., Yi, T., Tellides, G., Pober, J.S., Shkarin, P., Shapiro, E.M., Saltzman, W.M., Papademetris, X., Fahmy, T.M., and Breuer, CK. Initial evaluation of the use of USPIO cell labeling and noninvasive MR monitoring of human tissue-engineered vascular grafts *in vivo*. FASEB J **22,** 3888, 2008.
26. Melero-Martin, J.M., De Obaldia, M.E., Kang, S.Y., Khan, Z.A., Yuan, L., Oettgen, P., and Bischoff, J. Engineering robust and functional vascular networks *in vivo* with human adult and cord blood-derived progenitor cells. Circ Res **103,** 194, 2008.
27. Pittenger, M.F., Mackay, A.M., Beck, S.C., Jaiswal, R.K., Douglas, R., Mosca, J.D., Moorman, M.A., Simonetti, D.W., Craig, S., and Marshak, D.R. Multilineage potential of adult human mesenchymal stem cells. Science **284,** 143, 1999.
28. Kitamura, T., Onishi, M., Kinoshita, S., Shibuya, A., Miyajima, A., and Nolan, G.P. Efficient screening of retroviral cDNA expression libraries. Proc Natl Acad Sci USA **92,** 9146, 1995.
29. Melero-Martin, J.M., Khan, Z.A., Picard, A., Wu, X., Paruchuri, S., and Bischoff, J. *In vivo* vasculogenic potential of human blood-derived endothelial progenitor cells. Blood **109,** 4761, 2007.
30. Alencar, H., Mahmood, U., Kawano, Y., Hirata, T., and Weissleder, R. Novel multiwavelength microscopic scanner for mouse imaging. Neoplasia **7,** 977, 2005.
31. Hattori, H., Higuchi, K., Nogami, Y., Amano, Y., Ishihara, M., and Takase, B. A novel real-time fluorescent optical imaging system in mouse heart: a powerful tool for studying coronary circulation and cardiac function. Circulation **2,** 277, 2009.
32. Aikawa, E., Nahrendorf, M., Figueiredom, J.L., Swirski, F.K., Shtatland, T., Kohler, R.H., Jaffer, F.A., Aikawa, M., and Weissleder, R. Osteogenesis associates with inflammation in early-stage atherosclerosis evaluated by molecular imaging *in vivo*. Circulation **116,** 2841, 2007.
33. Cho, S.W., Kim, I.K., Kang, J.M., Song, K.W., Kim, H.S., Park, C.H., Yoo, K.J., and Kim, B.S. Evidence for *in vivo* growth potential and vascular remodeling of tissue-engineered artery. Tissue Eng **15,** 901, 2009.
34. Matsumura, G., Hibino, N., Ikada, Y., Kurosawa, H., and Shin'oka, T. Successful application of tissue engineered vascular autografts: clinical experience. Biomaterials **24,** 2303, 2003.
35. Matsumura, G., Ishihara, Y., Miyagawa-Tomita, S., Ikada, Y., Matsuda, S., Kurosawa, H., and Shin'oka, T. Evaluation of tissue-engineered vascular autografts. Tissue Eng **12,** 3075, 2006.
36. Shin'oka, T. [Clinical results of tissue-engineered vascular autografts seeded with autologous bone marrow cells]. Nippon Geka Gakkai Zasshi **105,** 459, 2004.
37. Kim, Y.S., Galis, Z.S., Rachev, A., Han, H.C., and Vito, R.P. Matrix metalloproteinase-2 and -9 are associated with high stresses predicted using a nonlinear heterogeneous model of arteries. J Biomech Eng **131,** 011009, 2009.
38. Zhang, J., Nie, L., Razavian, M., Ahmed, M., Dobrucki, L.W., Asadi, A., Edwards, D.S., Azure, M., Sinusas, A.J., and Sadeghi, M.M. Molecular imaging of activated matrix metalloproteinases in vascular remodeling. Circulation **118,** 1953, 2008.
39. Mason, D.P., Kenagy, R.D., Hasenstab, D., Bowen-Pope, D.F., Seifert, R.A., Coats, S., Hawkins, S.M., and Clowes, A.W. Matrix metalloproteinase-9 overexpression enhances vascular smooth muscle cell migration and alters remodeling in the injured rat carotid artery. Circ Res **85,** 1179, 1999.
40. Johnson, C., and Galis, Z.S. Matrix metalloproteinase-2 and -9 differentially regulate smooth muscle cell migration and cell-mediated collagen organization. Arterioscler Thromb Vasc Biol **24,** 54, 2004.
41. Galis, Z.S., and Khatri, J.J. Matrix metalloproteinases in vascular remodeling and atherogenesis: the good, the bad, and the ugly. Circ Res **90,** 251, 2002.
42. Athanasiou, K.A., Niederauer, G.G., and Agrawal, C.M. Sterilization, toxicity, biocompatibility and clinical applications of polylactic acid/polyglycolic acid copolymers. Biomaterials **17,** 93, 1996.
43. Hjortnaes, J., Bouten, C.V., Van Herwerden, L.A., Grundeman, P.F., and Kluin, J. Translating autologous heart valve tissue engineering from bench to bed. Tissue Eng Part B Rev **15,** 307, 2009.

Address correspondence to:
Elena Aikawa, M.D., Ph.D.
Center for Molecular Imaging Research
Massachusetts General Hospital
Harvard Medical School
149 13th St., Room 5420
Charlestown, MA 02129

E-mail: eaikawa@partners.org

Received: July 8, 2009
Accepted: September 11, 2009
Online Publication Date: October 26, 2009